ADVANCES IN INORGANIC CHEMISTRY, VOL. 38

NOVEL IRON–SULFUR CENTERS IN METALLOENZYMES AND REDOX PROTEINS FROM EXTREMELY THERMOPHILIC BACTERIA

MICHAEL W. W. ADAMS

Department of Biochemistry and Center for Metalloenzyme Studies, University of Georgia, Athens, Georgia 30602

I. Introduction
II. Extremely Thermophilic Bacteria
III. *Pyrococcus furiosus*
  A. Hydrogenase (Ni–Fe–S)
  B. Ferredoxin (Fe–S)
  C. Rubredoxin (Fe)
  D. Aldehyde Ferredoxin Oxidoreductase (W–Fe–S)
  E. Role of Fe–S Proteins in H_2 Production
IV. *Thermotoga maritima*
  A. Hydrogenase (Fe–S)
  B. Role of Tungsten
V. Summary
  References

I. Introduction

The aim of this article is to summarize the properties of a variety of Fe–S-containing proteins that have been purified from extremely thermophilic bacteria. Extreme thermophiles are defined as organisms that grow optimally at temperatures of 80°C and above. They are a relatively recent discovery in the microbial world. At the time we began this research in 1988, no metalloenzyme had been isolated from these bacteria. Since most of the extreme thermophiles metabolize molecular hydrogen (H_2), our initial objective was to characterize their hydrogenases, the enzymes responsible for catalyzing H_2 oxidation and H_2 production. Hydrogenases have been purified from several mesophilic organisms. All are thermolabile proteins containing Fe–S or Ni–Fe–S

centers. It was therefore of considerable interest to investigate the properties of enzymes capable of activating H_2 at temperatures near and above 100°C. Our initial research also led to the discovery that the growth of several extremely thermophilic bacteria is dependent upon tungsten (W), an element seldom used in biological systems. A new W–Fe–S-containing enzyme was subsequently purified, and its properties and proposed physiological role will also be described. The extreme thermophiles have also proved to be a rich source of more conventional Fe–S proteins, such as ferredoxin and rubredoxin. The properties of their Fe–S centers will also be discussed, both to emphasize their uniqueness and to demonstrate how they appear to be adapted to catalyze reactions and/or transfer electrons at temperatures near 100°C. As will become evident, extremely thermophilic Fe–S-containing proteins have distinct advantages over their mesophilic cousins. I begin with a brief description of the extremely thermophilic bacteria known at the present time.

II. Extremely Thermophilic Bacteria

As illustrated in Fig. 1 (*1–5*), that bacteria are able to grow optimally above 80°C is a recently discovered phenomenon. In 1982, Stetter (*6*)

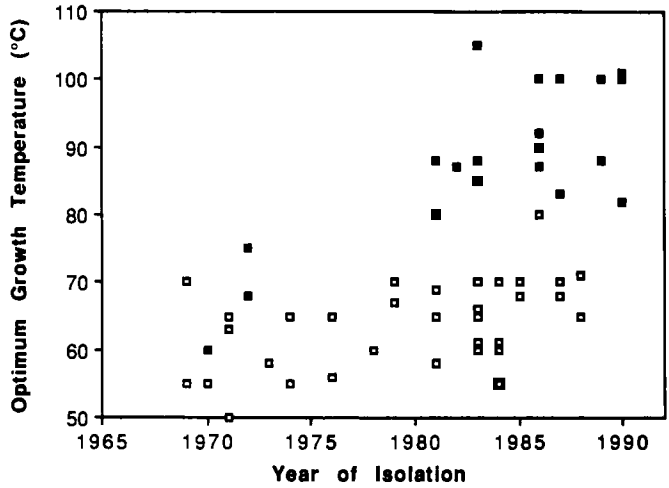

FIG. 1. The isolation of "thermophilic" bacteria over the last 20 years. Open symbols denote eubacteria in general; closed symbols are archaebacteria. Data taken from Refs. *1–5*.

first isolated a bacterium from shallow marine volcanic vents, his isolates grew at temperatures above 100°C. Since then, and due largely to the pioneering work of Stetter, almost 20 genera of bacteria able to grow near and above the normal boiling point of water have been isolated (*2–4*). All but one of these extremely thermophilic organisms are classified as archaebacteria; these are in contrast to the numerous thermophilic eubacteria that have been isolated over the years, most of which have growth temperature optima (T_{opt}) below 70°C (*5*). The one exception is the novel eubacterial genus, *Thermotoga* (*7*), which, in addition to being the most thermophilic, is also the most ancient eubacterium currently known (*7, 8*). Recent phylogenetic analyses (*9*) have also indicated that the extremely thermophilic archaebacteria and the eukaryotes have a common ancester, suggesting that extremely thermophilic organisms are the remnant of some form of universal ancestor to all extant life, having evolved when the earth was much hotter than it is at present (*8*). Phylogenetic implications of the metal dependence of bacterial growth will be considered in Section IV,B.

The majority of the extremely thermophilic organisms depicted in Fig. 1 have been found in geothermally heated marine environments, in both shallow (several meters below sea level) and deep water (several kilometers below sea level). Most of the extremely thermophilic archaebacteria are termed sulfur-dependent organisms, since, to a greater or lesser extent, they obtain energy for growth by the reduction or oxidation of elemental sulfur (S^0). Most grow anaerobically and reduce S^0 to H_2S, i.e., S^0 respiration, using either organic substrates or H_2 as the electron donor. They include the genera *Thermoproteus* (*10*), *Staphylothermus* (*11*), *Desulfurococcus* (*12*), *Thermofilum* (*13*), *Pyrobaculum* (*14*), *Acidianus* (*15*), *Desulfurolobus* (*16*), *Pyrodictium* (*17, 18*), *Thermodiscus* (*1*), *Pyrococcus* (*19, 20*), *Thermococcus* (*21, 22*), *Hyperthermus* (*23*), and the as-yet unclassified "ES-1" (*24*) and "ES-4" (*25*). Only species of *Desulfurolobus* and *Acidianus* are able to grow aerobically, and they do so by oxidizing S^0 to sulfuric acid. The remaining extremely thermophilic archaebacteria are strict anaerobes, and they comprise three methanogenic genera, *Methanopyrus* (*26*), *Methanococcus* (*27*), and *Methanothermus* (*28, 29*), and a unique sulfate-reducing genus, *Archaeglobus* (*30*). Species of the genera *Pyrococcus, Pyrobaculum, Pyrodictium, Hyperthermus,* and *Methanopyrus,* together with ES-4, grow optimally at or above 100°C, and the term "hyperthermophile" is usually used to refer to such organisms.

The dependence upon S^0 for optimal growth of most of the S^0-dependent, extremely thermophilic anaerobes means that they cannot be readily grown in large-scale stainless-steel fermentors because of the

corrosive nature of the H_2S that is generated. This problem is exacerbated by the high salt requirement of many of these marine organisms. However, some species are able to grow by fermentation: they are not obligately dependent upon S^0 respiration. They include the archaebacterium, *Pyrococcus furiosus,* and the extremely thermophilic eubacterium, *Thermotoga maritima.* Since these organisms also produce H_2 during growth, they were the obvious candidates with which to attempt the purification and characterization of metalloenzymes involved in H_2 metabolism. We now routinely grow each of these bacteria in 400-liter cultures and obtain cell yields of more than 600 g (wet weight) (*31, 32*). Purifications procedures are routinely carried out using at least 1 kg of cells, which gives sufficient quantities of the Fe–S-containing enzymes and proteins described below for various biochemical and spectroscopic analyses. All procedures are also performed under strictly anaerobic conditions and the procedures have been optimized to obtain all of the Fe–S proteins of one organism from the same batch of cells. The O_2 sensitivity (half-life in air) of the enzymes that have been purified varies from a few seconds for the hydrogenase of *T. maritima* to several hours for *P. furiosus* hydrogenase. The following descriptions of the various Fe–S proteins are organized based on their source. This permits a summary of their proposed physiological roles in *P. furiosus,* and how this differs in *T. maritima.*

III. *Pyrococcus furiosus*

Pyrococcus furiosus was isolated from a shallow marine volcanic vent by Fiala and Stetter in 1986 (*19*). It is a strictly anaerobic heterotroph that grows up to 105°C by the fermentation of carbohydrates such as starch and maltose to organic acids, CO_2, and H_2. The doubling time at its optimal growth temperature, 100°C, is around 40 min. As with most fermentative organisms, the H_2 produced inhibits growth, but this can be relieved either by sparging cultures with an inert gas to remove the H_2, or by adding S^0, which is reduced to H_2S. The latter reaction does not appear to conserve energy. Our initial studies with *P. furiosus* (*31*) showed that cell yields could be increased almost 10-fold by the presence of tungstate (10 μM) and of additional Fe in the growth medium. The role of W is discussed in Section III,D. The growth of *P. furiosus* was unaffected by the addition of salts of V, Cs, F, Pb, Rb, or Si, or by increased amounts (>10 μM) of Ni, Mo, Se, Co, or Mn.

A. HYDROGENASE (Ni–Fe–S)

Pyrococcus furiosus hydrogenase, the enzyme responsible for catalyzing the production of H_2 during the fermentative growth of this organism, is located in the cytoplasm and is routinely purified from cells grown in the absence of S^0 (*31*). It has a M_r value of around 185,000 and comprises three dissimilar subunits. It is one of the most thermostable enzymes known at present, having a half-life at 80°C of about 24 hr and an optimal temperature for catalysis above 95°C. This hydrogenase contains approximately 1 Ni, 30 Fe, and 24 acid-labile sulfide (S^{2-}) atoms/mole. Other metals, including W (and also Se), are not detected. The *P. furiosus* enzyme is different from the hydrogenases found in mesophilic bacteria that grow by fermentation and produce H_2, e.g., *Clostridium pasteurianum,* as these organisms contain a hydrogenase that lacks Ni (see Section IV,A). Ni–Fe hydrogenases are typically found in H_2-oxidizing bacteria, in which they are usually membrane bound and associated with an electron transport system that serves to couple H_2 oxidation with the reduction of a substrate, e.g., O_2. Most of the mesophilic Ni–Fe enzymes contain only two subunits ($\alpha\beta$) and immunological and DNA sequence analyses show extensive similarities between the enzymes from different bacterial genera (*33–35*). Some soluble Ni–Fe hydrogenases are known, and these usually have additional subunits that appear to function in the reduction of endogenous electron carriers, such as F_{420} in the methanogenic bacteria and NAD in the aerobic H_2-oxidizing bacteria (*36, 37*). The *P. furiosus* enzyme is similar in this respect, as it appears to contain an additional subunit that interacts with its physiological electron donor, which is a ferredoxin (see Section III,B). *Pyrococcus furiosus* hydrogenase does not use NAD(P)H as an electron carrier (*31*).

Mesophilic Ni–Fe hydrogenases are usually referred to as "uptake" hydrogenases, as their physiological role is H_2 oxidation and they catalyze only low rates of H_2 evolution in the standard *in vitro* assay system using dithionite-reduced methyl viologen as the electron donor. In contrast, mesophilic Fe hydrogenases are much more active enzymes, often by orders of magnitude. It was therefore surprising to find that the *in vitro* H_2 evolution activity of the *P. furiosus* enzyme (V_m = 2900 μmol evolved/min/mg or units/mg, at 80°C; Ref. *31*) was comparable to that obtained with Fe hydrogenases, e.g., V_m = 5500 units/mg at 30°C for *C. pasteurianum* hydrogenase I (*38*), rather than the Ni–Fe enzymes (V_m values typically < 100 units/mg at 30°C; Refs. *33* and *39*). In addition, all mesophilic hydrogenases (both Fe and Ni–Fe) preferentially catalyze H_2 oxidation when one compares the catalytic rates

of H_2 production with those obtained in H_2 oxidation assays using methylene blue or benzyl viologen as electron acceptors. The activity ratios (H_2 evolution/H_2 oxidation) are less than unity and typically 0.2–0.3 (see Ref. *4*). In contrast, the activity ratio for *P. furiosus* hydrogenase is approximately 4.0 between 45 and 80°C, and at 80°C remains more or less unchanged over the pH range 5–10. Moreover, above 80°C the activity ratio dramatically increases to around 12 at 95°C (*4, 31*). This change in catalytic activity at 80°C coincides with a transition point at 80°C in Arrhenius plots of enzyme activity, independent of the mode of assay. The *P. furiosus* enzyme therefore appears to be a new type of "evolution" hydrogenase. It is also well suited to its metabolic role, as it preferentially catalyzes H_2 evolution, the physiological reaction, at all temperatures, but especially above 80°C, at the growth temperature of *P. furiosus*.

Pyrococcus furiosus hydrogenase is purified anaerobically using buffers containing sodium dithionite (*31*). The electron paramagnetic resonance (EPR) spectra of the enzyme as isolated in its reduced state are shown in Fig. 2. The spectrum recorded at 70 K represents ~1 spin/mole and is typical of a single, reduced, and magnetically isolated $[2Fe–2S]^{1+}$ cluster. Below 15 K, the spectrum becomes more complex, indicating the presence of at least two interacting $[4Fe–4S]^{1+}$-type clusters with extremely rapid spin relaxation rates. The complete spectrum seen at 10 K represents approximately 2 spins/mole, suggesting that the 4Fe-type centers are not completely reduced under these conditions. There is no significant EPR absorption at lower magnetic fields (<3.0 T) so the reduced protein appears to contain only $S = \frac{1}{2}$ centers. These analyses therefore indicate that reduced *P. furiosus* hydrogenase contains one $[2Fe–2S]^{1+}$ cluster and at least one $[4Fe–4S]^{1+}$ cluster. All mesophilic Ni–Fe hydrogenases that have been examined to date contain at least two $[4Fe–4S]^{1+}$ centers (*33, 39, 40–42*), but 2Fe clusters have been detected only in the hydrogenases of some aerobic H_2-oxidizing bacteria, such as *Nocardia opaca* (*43*).

Pyrococcus furiosus hydrogenase is EPR silent upon anaerobic oxidation with thionine (E_m = + 11 mV; Refs. *4* and *31*). Thus, the majority of the Fe in this enzyme is not detected by EPR, as the 2Fe- and 4Fe-type centers account for at most 10 of its 30 Fe atoms. To investigate the possibility that the enzyme contained some unusual Fe–S center that was paramagnetic only at intermediate potentials, redox titrations were carried out using samples poised between −500 and +100 mV (at pH 8.0 and 20°C). However, no additional EPR signals were observed. The E_m value of the 2Fe cluster is estimated at −410 mV, whereas that of the 4Fe cluster(s) is −210 mV (Fig. 3), which is unusu-

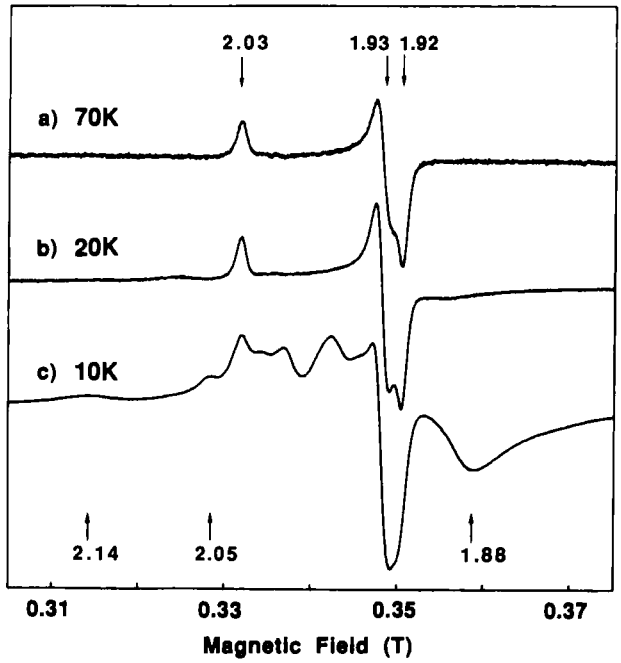

FIG. 2. EPR spectra of reduced *P. furiosus* hydrogenase. The hydrogenase (7.5 mg/ml) was under H_2 (1 atm) in 50 m*M* Tris/HCl buffer, pH 8.0, containing 1 m*M* sodium dithionite. The spectrometer microwave and power settings were (a and b) 2 mW and 5×10^5; (c) 50 mW and 4×10^4. The spectra were recorded at the indicated temperatures. Taken from Ref. *31*.

ally high for a ferredoxin-type center. These data also show that the 4Fe cluster(s) is completely reduced in the fully reduced protein: the intensity of the EPR signal remains constant between -300 and -500 mV (Fig. 3). The low-spin quantitation from the fully reduced enzyme is therefore not due to incomplete reduction of the 4Fe cluster(s).

Mesophilic Ni–Fe hydrogenases are purified aerobically and in this oxidized state they exhibit a characteristic EPR signal from the Ni center. Known as the Ni-A signal, this has g values of approximately 2.31, 2.23, and 2.02, and probably arises from a Ni(III) species (*33, 39, 40, 44*). This state is usually unable to catalyze H_2 oxidation without some form of reductive activation. The Ni-A EPR signal is lost during this process, and a transient EPR signal, termed Ni-C, is observed (g = 2.19, 2.16, and 2.02). The Ni-C signal is thought to arise from either a Ni(I) or Ni(III) species that has an E_m value of approximately

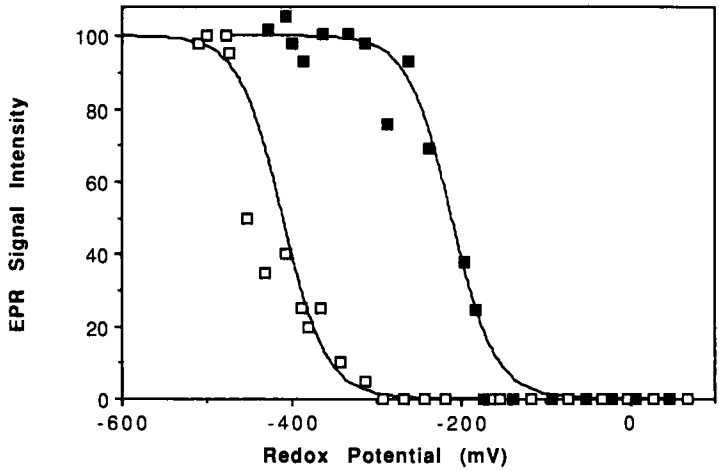

FIG. 3. Determination of the midpoint potentials of the 2Fe and 4Fe clusters in *P. furiosus* hydrogenase. The redox titration was carried out at 20°C and pH 8.0. The extent of reduction of the 4Fe cluster (closed symbols) and the 2Fe cluster (open symbols) was determined by the amplitudes of the $g = 1.88$ and $g = 2.03$ resonances (see Fig. 2), respectively (J.-B. Park and M. W. W. Adams, unpublished data, 1991).

−300 mV (*44–46*). In contrast, *P. furiosus* hydrogenase is purified anaerobically in a fully active state and remains active after oxidation with thionine, so it may not be expected to exhibit the Ni-A-type EPR signal. However, the mesophilic hydrogenases exhibit the Ni-C signal in the activated state, and it is therefore puzzling why a similar signal is not seen with the *P. furiosus* enzyme. Since this hydrogenase is virtually inactive at 20°C (see Fig. 4) (*47*), the temperature at which EPR samples are routinely prepared, it is possible that the Ni center can only be oxidized at higher temperatures. Our preliminary results suggest that this is indeed the case. An EPR signal reminiscent of the Ni-C signal is observed at approximately −300 mV when redox titrations are carried out at 80°C and samples are rapidly frozen for EPR analyses (J.-B. Park and M. W. W. Adams, unpublished data, 1991). The Ni site in this enzyme therefore appears to be inaccessible to redox mediators at ambient temperature, conditions under which its Fe–S centers are redox active. In contrast, a similar series of titrations focusing on the Fe–S clusters in this enzyme showed (1) that additional EPR signals are not apparent from samples prepared at high temperature, and (2) that the apparent E_m values of the 2Fe and 4Fe centers at 70°C are the same (±20 mV) as those measured from samples prepared

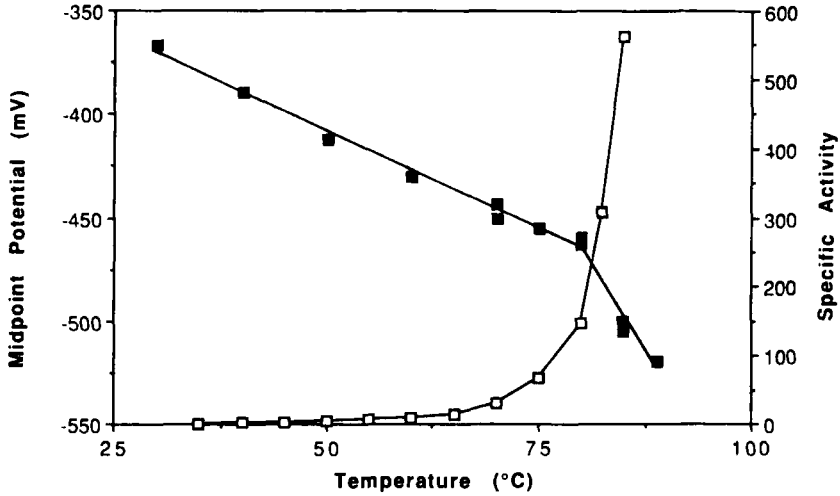

FIG. 4. Effect of temperature on the midpoint potential of *P. furiosus* ferredoxin and on the H_2 evolution activity catalyzed by *P. furiosus* hydrogenase using the ferredoxin as the electron donor. The midpoint potential data (closed symbols) are taken from Ref. *47*. The hydrogenase activity (open symbols) is expressed as micromoles H_2 evolved/min/mg of hydrogenase using dithionite-reduced ferredoxin at the indicated temperature. Taken from Ref. *31*.

at 20°C (Fig. 3). This is a very surprising result in view of the strong temperature dependence of the E_m values of Fe centers in other extremely thermophilic proteins (see Sections III,C–III,E).

It is therefore possible that the lack of significant catalytic activity of *P. furiosus* hydrogenase at low (ambient) temperature is because the Ni site is not accessible to the substrate (H^+ or H_2). It is assumed that the Fe–S clusters mediate electron transfer between the Ni site and the external electron carrier for the enzyme, so it is also likely that the Ni and Fe–S centers are not free to interact at low temperature, even though the Fe–S centers are accessible to redox mediators. It should be noted that the Ni site in the *P. furiosus* enzyme seems to be very different from that in the mesophilic enzymes. Not only does it preferentially catalyze H_2 evolution, it also has a unique response to the classical inhibitors of the mesophilic hydrogenases. For example, CO is a potent inhibitor of both Fe and Ni–Fe hydrogenases ($K_i \leq 30\ \mu M$; Ref. *33*) and the Ni–Fe, but not the Fe, enzymes, are also inhibited by acetylene (*4, 48*). Conversely, nitrite inhibits mesophilic Fe hydrogenases but it has little effect on the Ni–Fe enzymes (Ref. *33*; see also Section IV,A). In complete contrast, *P. furiosus* hydrogenase is insensitive to inhibition

by CO, nitrite, and acetylene (*4*). Since the Ni site appears inaccessible to both redox dyes and H_2/H^+ at 30°C, this might be expected, but the enzyme is also insensitive to all of these inhibitors at 80°C, conditions under which the properties of the Ni site more resemble those of the mesophilic enzymes.

Both the Fe–S and Ni centers in *P. furiosus* hydrogenase therefore have unusual properties when compared to their mesophilic counterparts. Of particular interest are the mechanisms by which the protein stabilizes the Ni site in the reduced state at low temperature (20°) and also maintains the midpoint potentials of the Fe–S centers independent of temperature (20–70°C). As described below, some of the redox proteins that have been isolated from *P. furiosus* promise to give some insight into the nature of the metal centers of the more complex enzymes such as *P. furiosus* hydrogenase.

B. Ferredoxin (Fe–S)

The physiological electron donor to the hydrogenase of *P. furiosus* hydrogenase is a ferredoxin (*49*). That is, *P. furiosus* ferredoxin acts as an electron carrier between sodium dithionite and *P. furiosus* hydrogenase in *in vitro* H_2 evolution assays. The hydrogenase has a high affinity for the ferredoxin: the apparent K_m value is 44 μM (*49*). However, as shown in Fig. 4, significant rates of H_2 production are observed only above 80°C, at the growth temperature of the organism. The ferredoxin also acts as an electron acceptor for the oxidation of pyruvate, glucose, and glyceraldehyde in *P. furiosus*, reactions catalyzed by three different oxidoreductases (see Sections III,D and III,E). Reduced *P. furiosus* ferredoxin also functions as an electron donor *in vitro* for H_2 evolution by the hydrogenase of the mesophile, *C. pasteurianum* (*49*). Although the apparent K_m value is very low (11 μM), the rate of H_2 evolution (V_m) is only 20% of that supported by *C. pasteurianum* ferredoxin.

Pyrococcus furiosus ferredoxin purified under anaerobic conditions (*49*) has an apparent molecular weight of ~7500 as determined by sedimentation analysis, which agrees with the value calculated from its amino acid sequence (M_r = 7148; J. B. Howard, J.-B. Park, and M. W. W. Adams, unpublished data, 1991). The protein contains a single $[4Fe–4S]^{1+/2+}$ cluster, and its UV-visible absorption spectrum is typical for a ferredoxin with a A_{390}/A_{280} ratio of 0.58 for the air-oxidized form. The molar absorbance coefficient at 390 nm is 15,400 M^{-1} cm^{-1}, and this decreases by 55% upon reduction with sodium dithionite. Interestingly, and in contrast to other ferredoxins, the reduction of *P. furio-*

sus ferredoxin by sodium dithionite is a time-dependent process at 23°C (taking ~20 min), although the reaction is immediate at 80°C. It is a remarkably thermostable protein: there are no changes in its spectroscopic properties (UV-visible and EPR) or in its electron carrier activity after a 12-hr incubation at 95°C (*49*). These data were obtained using the pure ferredoxin (0.5 mg/ml) in aqueous buffered solutions in the absence of any stabilizing agent. For comparison, the most "thermostable" ferredoxins previously reported are rapidly denatured (within minutes) at 85°C (*50–52*). *Pyrococcus furiosus* ferredoxin is also resistant to denaturants. There was no change in its spectroscopic properties and none of its iron became accessible to chelation after 3 hr at 23°C in the presence of sodium dodecyl sulfate (SDS) (20%, w/v). Similarly, a sample maintained in 6.0 *M* guanidinium hydrochloride containing 50 m*M* EDTA for 60 days at 4°C lost none of its iron. Iron is removed from the ferredoxin by prolonged acid treatment, but the apoprotein can be readily reconstituted by Fe^{2+} and S^{2-} to give a protein that was indistinguishable from the native protein in its stability and spectroscopic properties (*49*). The unusual stability of this protein is therefore an intrinsic property, and the novel spectroscopic properties of its cluster, described below, are not a purification artifact.

Ferredoxins containing [4Fe–4S] clusters have been purified from a wide range of bacteria, and over 30 amino acid sequences have been reported (*53–55*). Most of these proteins are of the 8Fe type and contain two [4Fe–4S] clusters. They have a consensus sequence of eight cysteinyl residues that binds the two clusters, invariably -$CX_2CX_2CX_3CP$-, in both halves of the molecule (*53*). As shown in Fig. 5, each cluster is coordinated by three cysteines of one-half of the molecule and by one cysteine (adjacent to the proline) in the other half. The few 4Fe ferredoxins known usually lack the fourth cysteine in one-half and up to three cysteines in the second half, but all maintain the 3 : 1 cysteine coordination to the cluster between the two halves of the molecule (Fig. 5). Alignment of the sequence of *P. furiosus* ferredoxin, however, shows that the second cysteine in the -$CX_2CX_2CX_3CP$- sequence is replaced by aspartate (corresponding to position 14 in the *P. furiosus* protein). The replacement of one coordinating cysteine by an aspartate is found in only four other ferredoxins (Fd), from *Desulfovibrio vulgaris* (*56*), *Desulfovibrio africanus* (Fd III; Ref. *57*), *Thermoplasma acidophilum* (*58*), and *Sulfolobus acidocaldarius* (*59*). However, all of these are 8Fe ferredoxins, leaving the *P. furiosus* protein as the only example of a 4Fe ferredoxin with incomplete cysteinyl coordination to its single [4Fe–4S] cluster. The likely ligand to the fourth iron atom of the cluster is discussed below.

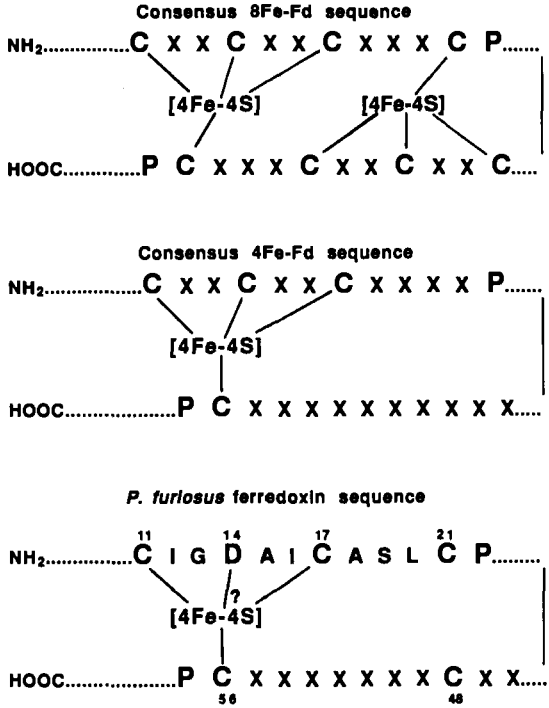

FIG. 5. Diagrammatic representation of the binding of [4Fe–4S] clusters to the consensus sequence of cysteinyl residues found in ferredoxins.

1. *Spectroscopic Characterization of the [4Fe–4S] Cluster*

a. Electron Paramagnetic Resonance Spectroscopy. Ferredoxins containing a single $[4Fe–4S]^{1+/2+}$ cluster give rise in their reduced states to a characteristic rhombic EPR signal below 30 K with typical g values of 2.08, 1.94, and 1.90 (*60*). A more complex spectrum arising from spin-interacting clusters is observed from the 8Fe proteins (*61*). Although reduced *P. furiosus* ferredoxin as prepared under anaerobic conditions exhibited a comparable EPR signal (Fig. 6) (*62*), the spectrum is much broader (g = 2.10, 1.87, and 1.80), it undergoes more rapid spin relaxation such that it is not observed above 15 K, and it represents only ~0.2 rather than 1 spin/molecule (*49, 62*). Furthermore, the reduced protein gives rise to additional EPR resonances at low field (g = 4.96 and 5.55; Fig. 6). The relative intensities of these resonances are strongly temperature dependent and arise from the upper and lower zero-field doublets of an $S = \frac{3}{2}$ ground state as interpre-

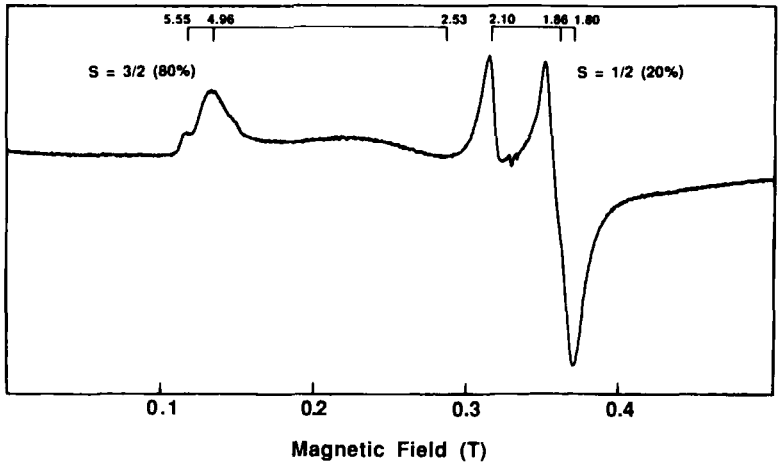

FIG. 6. EPR spectrum of reduced *P. furiosus* ferredoxin. The sample contained the ferredoxin (7 mg/ml) in 50 m*M* Tris/HCl buffer, pH 8.0, containing 2 m*M* sodium dithionite. The spectrum was recorded at 7 K using 10-mW microwave power. Modified from Ref. *62*.

ted by a conventional spin Hamiltonian ($E/D = 0.22, D = +3.3 \pm 0.2$ cm^{-1}; Ref. *62*). Spin determinations give a value of ~0.8 spin/mole for these low-field resonances. Q band EPR spectroscopy (at 35 GHz) of reduced *P. furiosus* ferredoxin showed resonances at the same g values as X band (at 9.3 GHz), confirming that the observed EPR absorption arises from a single magnetically isolated $[4Fe–4S]^{1+}$ cluster (*47*).

The $[4Fe–4S]^{1+}$ cluster in *P. furiosus* ferredoxin therefore exists with a spin mixture of $S = \frac{1}{2}$ (20%) and $S = \frac{3}{2}$ (80%) forms. Interestingly, comparable EPR properties were recently reported for the 8Fe ferredoxin of *D. africanus* (Fd III) in which one of the cysteine residues to one of its clusters is also replaced by aspartate (Ref. *63*; see also Armstrong, this volume). Although 4Fe clusters with a $S = \frac{3}{2}$ ground state have not been reported for any other ferredoxin, they are found in nitrogenase Fe protein (*64–66*), *C. pasteurianum* hydrogenase I (*67*), and glutamine phosphoribosylpyrophosphate amidotransferase (*68*). The coordinating ligands to the cluster in the hydrogenase are not known, but for the Fe protein and the amidotransferase there is substantial evidence for complete cysteinyl coordination (*68–71*). On the other hand, elegant studies by Beinert and co-workers have shown that one of the iron atoms of the $[4Fe–4S]^{1+}$ cluster of aconitase has noncysteinyl ligation and is coordinated by either H_2O or OH^-, but

this cluster exists in only a $S = \frac{1}{2}$ state (*72, 73*). Thus, noncysteinyl coordination of a specific iron atom of a $[4Fe–4S]^{1+}$ cluster is neither a prerequisite for, nor does not always lead to, an $S = \frac{3}{2}$ ground state. However, distinct differences do exist between the various $S = \frac{3}{2}$ clusters in their zero-field splitting parameters and in the ease with which they can be converted to the $S = \frac{1}{2}$ state. That of *P. furiosus* ferredoxin is so far unique in both aspects (*62*). For example, the two states of the cluster in this protein are very stable and are not interconverted by changes in the solvent media (*47*).

The E_m value of the [4Fe–4S] cluster in *P. furiosus* ferredoxin is -345 mV at 20°C and pH 8, as determined by redox titrations using EPR spectroscopy to monitor the extent of cluster reduction (*49*). This is comparable to but slightly more positive than the midpoint potentials of mesophilic ferredoxins (typically around -420 mV). There is no detectable difference between the redox properties of the $S = \frac{1}{2}$ and $S = \frac{3}{2}$ states of the 4Fe cluster in *P. furiosus* ferredoxin (*47*). Moreover, the E_m values of both states decrease linearly with increasing temperature, by -1.7 mV/°C over the range 20–80°C. As shown in Fig. 4, there appears to be a transition point at 80°C in the temperature dependence of the E_m value, with a change of approximately -6 mV/°C between 80 and 89°C (*47*). The E_m values and the relative amounts of the $S = \frac{1}{2}$ and $S = \frac{3}{2}$ forms of the cluster are also unaffected by pH (6.8–10.5), even at 85°C, and are unchanged in the presence of NaCl (1.0 *M*), sodium dodecyl sulfate (10%, w/v), or ethylene glycol (50%, v/v), even at 80°C (*47*). These results are quite remarkable for a biological system, as the redox potential and spin state of a [4Fe–4S] cluster are extremely sensitive monitors of the cluster environment, yet these appear to be unperturbed when the *P. furiosus* protein is subjected to extreme conditions.

In the redox titrations of *P. furiosus* ferredoxin, mediators were found to be superfluous at temperatures above 60°C (*47*), indicating that a mechanism exists for direct electron transfer between the Fe–S cluster of this relatively small protein and a platinum electrode. In contrast, the direct and preparative electrochemistry of mesophilic Fe–S proteins typically require the addition of "promoters," which modify the electrode surface and facilitate cluster–electrode interaction (*63, 74*). This temperature effect is so far unique to *P. furiosus* ferredoxin as *P. furiosus* rubredoxin does not interact directly with a platinum electrode, even at 90°C (see Section III,C). The results shown in Fig. 4 also allow an estimation of the E_m value of *P. furiosus* ferredoxin at 100°C, at the growth temperature of the organism. By extrapolation, it is less than -550 mV, and possibly as low as -600 mV. Notably, the change in

the temperature dependence of the E_m value of the ferredoxin at 80°C corresponds with the tremendous increase in the rate of H_2 evolution above 80°C catalyzed by *P. furiosus* hydrogenase when the ferredoxin is the electron carrier (Fig. 4). A similar temperature effect on H_2 production is not observed with artificial electron carriers, e.g., methyl viologen, and the hydrogenase (*31*). Therefore, the redox potential of the ferredoxin may in some way limit the rate of electron transfer to the hydrogenase (and thus H_2 production) at temperatures below 80°C.

b. Electron–Nuclear Double Resonance. The question arises as to what differentiates the two spin states ($S = \frac{1}{2}$ and $S = \frac{3}{2}$) of the $[4Fe–4S]^{1+}$ cluster in *P. furiosus* ferredoxin. One explanation is that the two states are in thermodynamic equilibrium at the temperature at which the EPR spectra are recorded. This is not the case, however, as one would expect the relative intensities of the EPR signals of the two states to change between 4 and 15 K, but they remain constant over this temperature range (*62*). The two spin states must therefore reflect different conformations of a [4Fe–4S] cluster, which themselves must be maintained by different structures of the protein. Electron–nuclear double-resonance (ENDOR) spectroscopy was used to determine if these structural differences were manifested by an inequivalence between the two forms of magnetically coupled protons. ENDOR is a double-resonance technique that provides information on the type and number of nuclei (where $I \neq 0$) that are part of or interact with an EPR-active paramagnetic center, e.g., Ref. *72*. As shown in Fig. 7, multiple ^1H ENDOR resonances were detected at the $g = 1.84$ EPR resonance ($S = \frac{1}{2}$) of *P. furiosus* ferredoxin (*47*). These correspond to hyperfine coupling constants of 4–6 MHz. Similar resonances have been observed with other reduced ferredoxins and they are assigned to the methylene protons of the cysteinyl residues that bind the $[4Fe–4S]^{1+}$ cluster. However, the *P. furiosus* protein also exhibited a ^1H ENDOR resonance corresponding to a coupling constant of ~22 MHz (Fig. 7). Such a strongly coupled proton has not been reported for any other Fe–S protein. Moreover, when the ferredoxin is in D_2O, the weakly coupled protons remain unchanged, as expected, but the 22-MHz resonance is not observed (Fig. 7). Instead, a single ^2H ENDOR resonance is seen showing that D_2O interacts directly with the paramagnetic center (*47*). A surprising result was obtained upon examination of the $g = 3.60$ EPR absorption ($S = \frac{3}{2}$) from *P. furiosus* ferredoxin. This showed similar although not identical ENDOR resonances from weakly coupled protons and also a strongly coupled resonance ($A \leq 20$ MHz), but the latter was unaffected when the ferredoxin was examined in D_2O (*47*). The

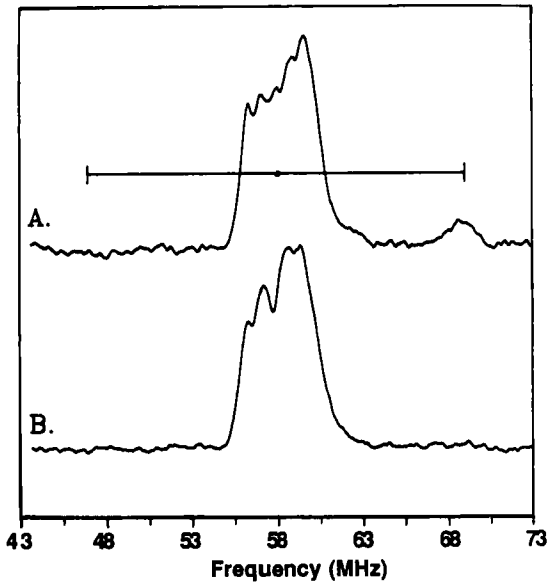

FIG. 7. Q band ^{1}H ENDOR of the $S = \frac{1}{2}$ form of the [4Fe–4S]$^{1+}$ cluster of *P. furiosus* ferredoxin. Samples of the ferredoxin (10.7 m*M*) were prepared in H_2O (A) and in D_2O (B). Spectra were recorded using a microwave frequency of 35.39 GHz and power of 0.05 mW at 2 K. The magnetic field was set at 1.375 T ($g = 1.84$). Taken from Ref. *47*.

solvent accessibility of the [4Fe–4S]$^{1+}$ cluster therefore appears to be very different in the $S = \frac{1}{2}$ and $S = \frac{3}{2}$ ground states.

The two spin forms of the [4Fe–4S]$^{1+}$ cluster in *P. furiosus* ferredoxin can therefore be differentiated by the exchangeability (in the $S = \frac{1}{2}$ form) or nonexchangeability (in the $S = \frac{3}{2}$ form) of a water-derived hydrogen atom that directly interacts with the 4Fe cluster, an interaction not seen in other 4Fe ferredoxins. This hydrogen atom appears to be derived from OH^- rather than H_2O, as the EPR and redox properties of the protein were unchanged over the pH range 6.8–10.5 (*47*). The obvious conclusion is that these unique properties are associated with the lack of complete cysteinyl ligation to the [4Fe–4S]$^{1+}$ cluster of this protein, and suggest that an OH^- molecule directly coordinates to the unique fourth Fe atom. This is shown diagrammatically in Fig. 8. The coordination of OH^- (or H_2O) to a unique Fe site of the [4Fe–4S]$^{1+}$ cluster of aconitase has been established by crystallographic studies (*75*). However, as well as exclusively exhibiting an $S = \frac{1}{2}$ ground state (72), the D_2O-exchangeable ^{1}H ENDOR resonances associated with this cluster have *A* values $\leq$8 MHz, much less than that observed with *P.*

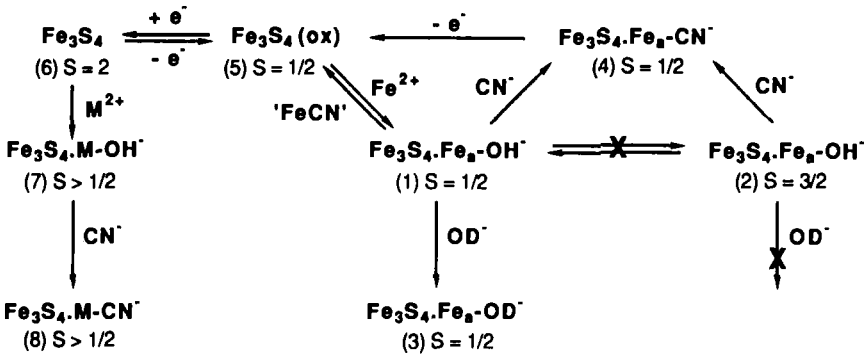

FIG. 8. Proposed reactions of the unique noncysteinyl Fe atom (Fe_a) in the [4Fe–4S] cluster of *P. furiosus* ferredoxin. In the native protein the cluster (1 and 2) has OH^- bound, but only in the $S = \frac{1}{2}$ state (1) can this exchange with OD^- (3). Both spin states react with cyanide (4). The 3Fe cluster (5) is generated by ferricyanide ("FeCN") treatment of (1) and (2) or by oxidation (> -100 mV) of (4). The Fe_a atom can be substituted by the addition to (6) of a metal ion, M (Ni, Co, or Zn). This is assumed also to bind OH^- (7) and M can also bind cyanide (8). All clusters except (5) are in their reduced forms and the spin state of each is indicated.

furiosus ferredoxin (*76, 77*). The differences between the 4Fe clusters of aconitase and *P. furiosus* ferredoxin may lie with the role of the amino acid side chain that replaces the expected cysteinyl group. In aconitase, which lacks the consensus sequence of cysteinyl residues found in the ferredoxins, there is no residue in the immediate vicinity of the unique Fe atom (*75, 76*). This may not be the case with the aspartyl group that replaces the cysteinyl residue in *P. furiosus* ferredoxin, although as yet there is no information as to whether this aspartyl residue interacts with the fourth Fe atom of the cluster.

A question then remains: why is the OH^- molecule bound to the $[4Fe–4S]^{1+}$ cluster in *P. furiosus* ferredoxin exchangeable in the $S = \frac{1}{2}$ form but not in the $S = \frac{3}{2}$ form? This would suggest that significant structural changes exist between the two ground states involving the adjacent amino acid residues, whereby the cluster is shielded from the solvent in the $S = \frac{3}{2}$ but not in the $S = \frac{1}{2}$ form. This then raises the question of what aspects of the protein structure determines which of the two forms predominate. Obviously this is an intrinsic property of the protein, since the reconstituted ferredoxin (after acid precipitation) has the same $S = \frac{1}{2}$ to $S = \frac{3}{2}$ ratio as the native protein (*49*). Similarly, the factors that contribute to one form or the other are exceedingly stable, unaffected by high temperature, pH extremes, and denaturants. As yet there is no information as to what these factors might be. Since

synthetic clusters of the [4Fe–4S–4(SR)] type have been shown to exist in mixtures of $S = \frac{1}{2}$ and $S = \frac{3}{2}$ spin states (in frozen dimethylformamide solution; Ref. *78*, see also Holm, this volume), detailed structural studies of *P. furiosus* ferredoxin using, for example, NMR and crystallography, may yield information on this unsolved aspect of Fe–S cluster chemistry.

c. Magnetic Circular Dichroism and Resonance Raman Spectroscopy. Variable-temperature magnetic circular dichroism (MCD) is a particularly powerful spectroscopic technique in discriminating paramagnetic Fe–S clusters and in providing information on their electronic properties (see Refs. *67, 79,* and *80*). Thus, the MCD data of reduced *P. furiosus* ferredoxin were in accord with its EPR properties and showed that its cluster is of the 4Fe type with a predominant $S = \frac{3}{2}$ ground state (*62*). In resonance Raman spectroscopy, the bands observed correspond to stretching vibrations of bridging and terminal Fe–S bonds within an Fe–S cluster, the frequencies and intensities of which are very diagnostic of cluster type. Hence, the bands observed with oxidized *P. furiosus* ferredoxin (*62*) were very similar to those seen from $[4Fe–4S]^{2+}$ clusters in other ferredoxins (*81, 82*). The latter have been rigorously assigned to predominantly terminal (Fe-cysteinyl) or bridging Fe–S stretching by extensive studies using synthetic analogs, isotope shifts (with ^{54}Fe and ^{34}S), and normal mode calculations. The most significant difference in the Raman spectrum of *P. furiosus* ferredoxin is in the totally symmetric bridging vibration, which is the dominant feature in the Raman spectrum. In proteins and also in synthetic clusters that contain a $[4Fe–4S]^{2+}$ cluster with complete cysteinyl (or thiolate) coordination, the totally symmetric bridging frequencies range between 333 and 338 cm^{-1} (*62, 81, 82*). That of *P. furiosus* ferredoxin is shifted to higher energy and is seen at 342 cm^{-1}. Interestingly, a similar shift is also seen with the $[4Fe–4S]^{2+}$ clusters of aconitase (340 cm^{-1}) and sulfite reductase (342 cm^{-1}), both of which have a unique Fe site that arises because of atypical coordination. As noted above, this is H_2O/OH^- in the case of aconitase (*76*), but an unknown ligand bridges between the siroheme and the 4Fe cluster in sulfite reductase (*83*). This site differentiation appears to lower the cluster symmetry (from D_{2d} to C_{3v}) and shift the totally symmetric bridging frequencies closer to those seen from $[3Fe–4S]^{1+}$ clusters, which are typically 347–348 cm^{-1} (*82*). The frequency of the totally symmetric bridging vibration may therefore prove to be a useful indicator of site differentiation in 4Fe clusters, arising from anomalous coordination to one Fe atom.

2. *Spectroscopic Characterization of the [3Fe–4S] Cluster*

Oxidation of anaerobically purified *P. furiosus* ferredoxin (with O_2, thionine, or 2,6-dichlororphenolindophenol) does not result in degradation of its cluster, but oxidation with a fivefold excess of potassium ferricyanide shows quantitative conversion of the $[4Fe–4S]^{1+}$ cluster to a $[3Fe–4S]^{1+}$ cluster (Fig. 8; Refs. *49* and *62*). The EPR (Fig. 9), variable-temperature MCD, and resonance Raman spectra of the fer-

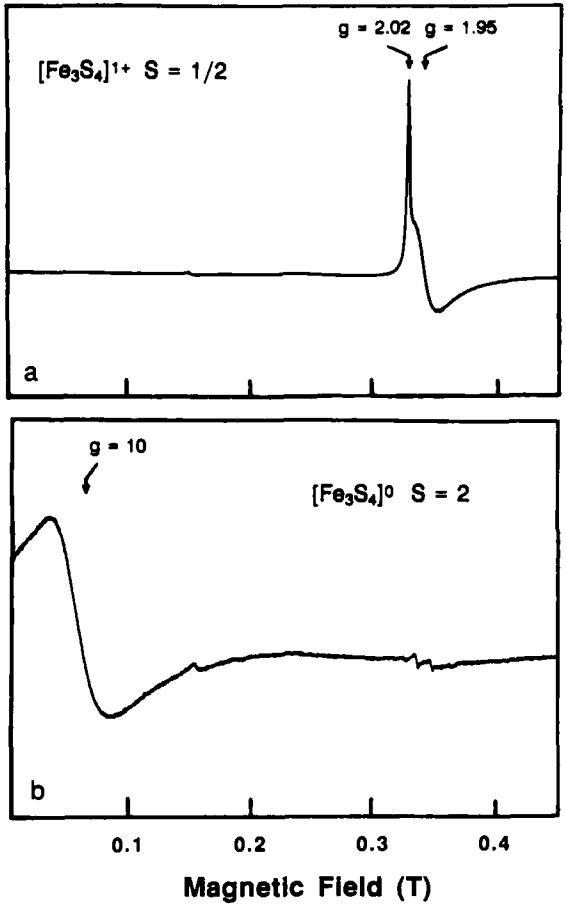

FIG. 9. EPR spectra of the oxidized (a) and reduced (b) states of the [3Fe–4S] cluster in *P. furiosus* ferredoxin. The sample concentration was 3 mg/ml and spectra were recorded at 8 K. The microwave power used was 1 mW (oxidized) and 50 mW (reduced). Modified from Ref. *62*.

ricyanide-treated protein are all very similar to those of $S = \frac{1}{2}$ $[3Fe–4S]^{1+}$ clusters in other bacterial ferredoxins (*62*). EPR-monitored redox titrations indicate an E_m value of -160 mV (at pH 8.0 and 23°C) for the 3Fe center in *P. furiosus* ferredoxin (*49*). Upon reduction of the 3Fe ferredoxin with sodium dithionite, the only feature in its EPR spectrum is a broad derivative-shaped feature at $g = 10$ arising from transitions within a $M_s = \pm 2$ doublet of an $S = 2$ ground state (Fig. 9). In addition, MCD magnetization studies of the reduced 3Fe protein were only interpretable in terms of an $S = 2$ ground state with a negative axial zero-field splitting parameter, $D < 0$ (*62*). The intensity and form of the low-temperature MCD spectrum also indicates the presence of one $[3Fe–4S]^0$ cluster (*62*). Moreover, recent data from a saturation magnetization study are also consistent with one reduced 3Fe cluster per protein molecule. The fit parameters were $S = 2$, $D = -3\ cm^{-1}$, $E/D = 0.23$, and $g = 2.10$ (E. P. Day, J.-B. Park, and M. W. W. Adams, unpublished data, 1991). The $[3Fe–4S]^{0/1+}$ cluster in *P. furiosus* ferredoxin therefore has structural, electronic, and magnetic properties analogous to those in mesophilic 3Fe ferredoxins in both the oxidized and reduced states. Since the 4Fe cluster in this protein has unusual spectroscopic properties, it would seem likely that the Fe atom that is removed on formation of the [3Fe–4S] cluster is the one that has noncysteinyl coordination. This is further supported by comparisons with the 3Fe form of the ferredoxin from *D. gigas*. This has the consensus sequence of cysteinyl residues and the one that is equivalent to the aspartyl residue in *P. furiosus* ferredoxin is the one that is not involved in coordinating the 3Fe cluster (*84, 85*).

A stoichiometric amount of a conventional [3Fe–4S] cluster can therefore be readily generated in *P. furiosus* ferredoxin by a facile procedure, and all of the spectroscopic data indicate that there is no residual [4Fe–4S] cluster (*62*). Indeed, even after incubating the 3Fe ferredoxin at 80°C for 4 days, there was no evidence of cluster destruction or conversion to the 4Fe form. However, as noted above, quantitative cluster conversion is easily accomplished by adding stoichiometric amounts of Fe(II) under reducing conditions to yield [4Fe–4S] clusters with spectroscopic characteristics identical to those of the anaerobically purified protein (*47, 62*). This ease of cluster interconversion (both 4Fe to 3Fe and vice versa) is comparable to what has been found with aconitase (*86*), which, as discussed above, also has noncysteinyl ligation to the removable Fe atom (*76*). On the other hand, cluster conversion is much more difficult with mesophilic ferredoxins having total cysteinyl coordination. For example, the 4Fe clusters of *C. pasteurianum* ferredoxin tend to degrade rather than form 3Fe clusters (*87*). Similarly, *D.*

gigas ferredoxin can be purified as either the 3Fe or 4Fe form, and although the two can be interconverted, there is evidence for some cluster degradation and the presence of apoprotein (*88*). The presence of a single 4Fe cluster and quantitative cluster interconversion, coupled with extreme stability, makes *P. furiosus* ferredoxin an attractive model system with which to not only investigate the electronic and magnetic properties of Fe–S centers, but also their reactivity. This includes both to small molecules and to the incorporation of other metal ions to generate mixed-metal clusters.

3. *Ferredoxin as a Model of Enzymatic Fe–S Clusters*

Before considering the potential of *P. furiosus* ferredoxin as an analog of the active sites of Fe–S enzymes, it is necessary to summarize what is known about "catalytic" Fe–S clusters. Indeed, the notion that Fe–S clusters fulfill functions other than simple electron transfer is a fairly recent development in the Fe–S protein field. Although some Fe–S-containing enzymes contain a [4Fe–4S] cluster of no known function, e.g., endonuclease III (*89*) and glutamine phosphoribosylpyrophosphate amidotransferase (*90*), in some others, Fe–S clusters bind small molecule substrates and appear to participate in catalyzing chemical reactions. Since ferredoxin-type [4Fe–4S] (and [2Fe–2S]) clusters do not bind small molecules or catalyze any known chemical reaction (*91, 91a*), the question arises as to how such clusters have been "activated" or "functionalized" in Fe–S-containing enzymes such that they can bind and activate substrates. Two mechanisms appear to exist from the Fe–S enzymes studies so far. The first is by replacing one or more of the cysteinyl sulfur ligands that bind the Fe–S cluster to the protein. Into this group fall the hydratases, of which the tricarboxylic acid cycle enzyme, aconitase, is the prototypical example. Beinert and co-workers (*75, 76*) have shown that in addition to OH^-/H_2O, the non-sulfur-ligated Fe atom of its single [4Fe–4S] cluster can bind the substrates citrate or *cis*-aconitate. Several other hydratases (or hydrolases) have also been shown to contain Fe–S clusters and presumably these function in a similar fashion (*92–96*). Besides hydratases, there are so far only two examples of enzymes containing Fe–S clusters with partial nonsulfur ligation, and both are involved in catalyzing redox reactions. One is nitrogenase, which is discussed below, and the other example is Fe hydrogenases. As described in Section IV,A, the H_2-activating center of the Fe hydrogenases is thought to be a novel Fe–S cluster, termed the H cluster (see Ref. *38* for review). A recent study showed that the H cluster of hydrogenases I from *C. pasteurianum* contains two distinct types of nitrogenous ligands (*97*), although the extent to which these

ligands participate in or enable catalysis by the H cluster is as yet unknown.

The second mechanism by which [4Fe–4S]-type clusters could be modified so that they can catalyze chemical reactions is by the replacement of one of the Fe atoms by a second type of metal. There are two enzymes that may fit into this category. The first is nitrogenase, which contains a dissociable Mo–Fe–S cluster at the site of N_2 reduction. Of stoichiometry $Fe_{6-8}S_{8-10}Mo$ (*98, 99*), this appears to contain a [Mo–3Fe] unit (*100, 101*), and similar [V–3Fe] and ["Fe"–3Fe] cores are thought to be present in the alternative vanadium- and iron-containing nitrogenases (*102–104*). As noted above, nonsulfur ligands to these Fe–S clusters may also play a role in their catalytic abilities, since ESEEM spectroscopy has been used to show that the Mo–Fe–S cluster of the molybdenum nitrogenase has a degree of N coordination (*105*). The second enzyme that may contain a mixed-metal Fe–S cluster is the CO dehydrogenase of acetogenic, methanogenic, and photosynthetic bacteria (*106–111*). For example, a recent ENDOR study (*112*) concluded that when *Clostridium thermoaceticum* CO dehydrogenase is reacted with CO, a mixed metal–carbon complex of stoichiometry $NiFe_{3-4}S_{\geq 4}C$ is generated. The data were consistent with either a [Ni–3Fe–4S] cluster or a mononuclear Ni bridged by a ligand to a $[4Fe–4S]^{1+}$ cluster as the source of the novel $S = \frac{1}{2}$ EPR resonance ($g_{\parallel} = 2.03, g_{\perp} = 2.07$) induced by CO treatment. Mössbauer data from the same enzyme (*113*) rule out a 3Fe-type center at the active site of this enzyme, unless another metal (M)—and Ni or Fe are the obvious choices—is incorporated into the site to give an M–3Fe–4S-type structure.

Enormous insight into the properties of biological Fe–S clusters and potential models of them have come from purely synthetic approaches. Largely through the work of Holm and co-workers, their synthesis and characterization has opened up a new area of inorganic chemistry (for example, see Refs. *91, 114–118*). However, synthetic analogs are characterized in nonaqueous media, which does not easily allow one to mimic the chemical environment of a protein, and their redox properties, an essential parameter for comparisons with biological clusters, are frequently ill-defined and hard to translate to aqueous media. Also, no synthetic Fe–S cluster catalyzes a chemical reaction (some will generate H_2 and reduce C_2H_2, but in less than stoichiometric amounts; Ref. *119*). In contrast to the synthetic analogs, Fe–S clusters in proteins afford a totally aqueous system and offer enormous potential for varying both ligands to specific sites of the cluster and the chemical environment of the cluster. In addition, functional amino acid groups likely to

participate in catalysis can be added at strategic points adjacent to the cluster (although a major disadvantage with proteins is that crystal structures cannot be as readily obtained as they can with synthetic analogs). The diversity in properties of enzymatic [4Fe–4S]-type clusters and their apparent catalytic potential make 4Fe ferredoxins the obvious choice for a model system, with the added prerequisite of facile 4Fe to 3Fe conversion. For example, the fourth site of the [3Fe–4S] cluster in *D. gigas* ferredoxin can be occupied by other divalent metals, namely, zinc or cobalt (*120, 121*). Although of no known biological relevance, spectroscopic data show that these $[M–3Fe–4S]^{1+}$ clusters (where M = Co or Zn) are extremely useful in understanding intracluster magnetic interactions. However, the presence of a cysteinyl residue adjacent to the "vacant" site of the 3Fe cluster might be expected to hinder attempts at incorporating other metals, and cysteinyl coordination to the fourth Fe atom in a [4Fe–4S] cluster would preclude binding of exogenous ligands. In the following discussion it is shown that these difficulties do not arise with *P. furiosus* ferredoxin, owing to the presence of partial noncysteinyl ligation to its Fe–S cluster.

a. Formation and Properties of the [Ni–3Fe–4S] Cluster. The [Ni–3Fe–4S] cluster was generated in *P. furiosus* ferredoxin using procedures similar to those used by Münck and co-workers for incorporating Zn(II) and Co(II) into the [3Fe–4S] core of *D. gigas* ferredoxin to give [Zn–3Fe–4S] and [Co–3Fe–4S] clusters (*120, 121*). It is prepared by incubating dithionite-reduced 3Fe ferredoxin in 100 m*M* Mes buffer, pH 6.0, with a 20-fold excess of $NiCl_2$ under anaerobic conditions for 15 min at 23°C (*122*). Excess Ni(II) can be removed by treatment with EDTA and subsequent gel filtration under anaerobic conditions. As shown in Fig. 10b, incorporation of Ni(II) into the $S = 2$ $[3Fe–4S]^0$ cluster yields a ground state with half-integer spin. This is analogous to the incorporation of Fe(II) into the 3Fe core, as this gives the $S = \frac{1}{2}$ and $S = \frac{3}{2}$ mixture of the $[4Fe–4S]^{1+}$ cluster (Fig. 10a). Thus, the binding of an M^{2+} ion (M = Fe, Ni) is accompanied by a one-electron reduction of the 3Fe cluster to the $[M–3Fe–4S]^{1+}$ state. However, in contrast to the $[Zn–3Fe–4S]^{1+}$ of *D. gigas* ferredoxin, which has an $S = \frac{5}{2}$ ground state (*121*), the Ni analog is an $S = \frac{3}{2}$ species. Its spectrum comprises positive maxima at $g = 5.7$ and 4.9, a broad derivative centered at $g = 2.9$, and a weak negative feature at $g = 1.8$. These resonances can be rationalized using a spin Hamiltonian with an isotropic Zeeman interaction. For example, with $E/D = 0.18, D < 0$, and $g_0 = 2$, the $S = \frac{3}{2}$ spin Hamiltonian predicts $g(x, y, z) = 2.88, 4.95$, and 1.84 and 1.12, 0.94, and 5.82 for the upper and lower doublets,

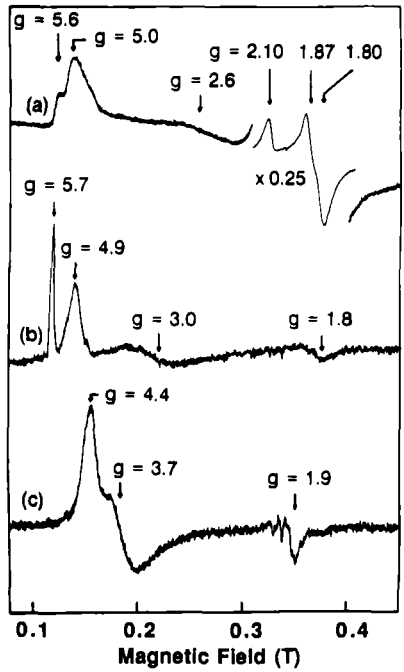

FIG. 10. EPR spectra of the $[Ni–3Fe–4S]^{1+}$ cluster in *P. furiosus* ferredoxin and the cyanide-bound form. The samples were as follows: (a) reduced ferredoxin (3.5 mg/ml) containing a $[4Fe–4S]^{1+}$ cluster; (b) reduced ferredoxin (2.5 mg/ml) containing a $[Ni–3Fe–4S]^{1+}$ cluster; (c) after treatment of sample b with a 50-fold excess of potassium cyanide. Temperatures and microwave powers used: (a) 8 K, 10 mW; (b) 4.5 K, 50 mW; (c) 7 K, 1 mW. Taken from Ref. *122*.

respectively. The temperature dependence of the low-field EPR signals shows that the $g = 5.7$ and 4.9 components originate from the lower and upper doublets, respectively. Therefore, the zero-field splitting is opposite in sign compared to the $S = \frac{3}{2}$ $[4Fe–4S]^{1+}$ center (Fig. 10a). Analysis of the intensity ratio of the $g = 5.8$ and $g = 4.9$ features as a function of $1/T$ indicates $D = -2.2 \pm 0.2$ cm^{-1} (*122*). Preliminary variable-temperature MCD analyses of the $[Ni–3Fe–4S]^{1+}$ cluster of *P. furiosus* ferredoxin show a temperature-dependent spectrum that is distinct from the dithionite-reduced native 4Fe form (*62*), and the magnetization data are consistent with the EPR-determined ground state properties (R. C. Conover, J.-B. Park, M. W. W. Adams, and M. K. Johnson, unpublished data, 1991). It should be noted that Münck and co-workers (*123*) observed EPR resonances similar to those shown

in Fig. 10b during studies of the reaction of Ni(II) with the 3Fe form of *D. gigas* ferredoxin.

Evidence for the presence of a [Ni–3Fe–4S]$^{1+}$ cluster in *P. furiosus* ferredoxin comes from two sources. First, the $g = 5.7$ shown in Fig. 10b is broadened when ^{61}Ni ($I = \frac{3}{2}$) is used (*122*), showing that the observed spectroscopic changes involve the incorporation of Ni into the paramagnetic center. Second, a [Ni–3Fe–4S]$^{1+}$ cluster was recently synthesized and characterized by Holm, Münck, and co-workers (Ref. *124*; see Holm, this volume). The cuboidal nature of the cluster was evident from crystallographic analysis that showed a Ni–Fe distance of 2.69 Å, analogous to the Fe–Fe distances (~2.7 Å) in both synthetic and biological [4Fe–4S] clusters. The synthetic [Ni–3Fe–4S]$^{1+}$ cluster also has a $S = \frac{3}{2}$ ground state and exhibits EPR properties similar to those of the Ni-incorporated 3Fe form of *P. furiosus* ferredoxin. These data clearly show that the synthetic and protein-bound Ni–Fe clusters are structurally similar.

So, do the spectroscopic properties of the [Ni–3Fe–4S] cluster in *P. furiosus* ferredoxin in any way resemble those reported for the Ni–Fe site in CO dehydrogenase? As noted above, the Ni–Fe complex in CO-treated *C. thermoaceticum* CO dehydrogenase exhibits a novel $S = \frac{1}{2}$ EPR resonance, but this is only observed upon CO reduction and it is a relatively minor component, typically accounting for only 0.15 spin/Ni (*113*). Furthermore, ill-defined $S = \frac{3}{2}$ EPR signals centered around $g = 5$ are apparent from both the dithionite- and CO-reduced enzyme. Similarly, EPR signals near $g = 4.3$ from a $S > \frac{1}{2}$ center as well as a $S = \frac{1}{2}$ resonance ($g = 2.04$, 1.90, and 1.71) have been assigned to the Ni–Fe center in the CO dehydrogenase from *Rhodospirillum rubrum* (*110*). It is therefore possible that the majority of the active sites in these enzymes have a Ni–Fe complex with an $S = \frac{3}{2}$ ground state, although it remains to be seen if this has a structure analogous to the Ni–3Fe cluster in *P. furiosus* ferredoxin.

b. Exogenous Ligand Binding to the [M–3Fe–4S] Clusters. Cyanide is a potent competitive inhibitor of all known CO dehydrogenases (*125*), so it was of great interest to investigate the possibility of cyanide binding to the [Ni–3Fe–4S]$^{1+}$ center in *P. furiosus* ferredoxin. As shown in Fig. 10, the addition of a 50-fold excess of cyanide to the Ni-substituted protein results in the complete conversion of the $S = \frac{3}{2}$ [Ni–3Fe–4S]$^{1+}$ EPR spectrum (Fig. 10b) to a new EPR signal (Fig. 10c; see Ref. *103*). The g values (4.4, 3.7, and 1.9) indicate an axial $S = \frac{3}{2}$ species ($E/D = 0.06$), and temperature-dependence studies (4–15 K) show that this resonance arises exclusively from the lower Kramers'

doublet, i.e., $D > 0$ (*122*). Further studies to conclusively establish that Ni is the cyanide-binding site and the spectroscopic consequences of binding other ligands to the $[Ni–3Fe–4S]^{1+}$ cluster in *P. furiosus* ferredoxin are in progress. Interestingly, it may be of relevance to note that synthetic mixed-metal clusters containing $[V–3Fe–4S]^{2+}$, $[Mo–3Fe–4S]^{3+}$, and $[W–3Fe–4S]^{3+}$ cores, and the nitrogenase Fe–Mo cofactor (*91, 126*), all exhibit $S = \frac{3}{2}$ ground states with EPR characteristics remarkably similar to those of the cyanide-bound $[Ni–3Fe–4S]^{1+}$ ferredoxin (*122*).

We now return to the notion that reactivity (and catalytic activity) in biological Fe–S clusters can also be imparted by the presence of nonsulfur ligation to one of the Fe sites of a 4Fe cluster. The results described in Section III,B,1 indicate that the unique Fe atom of *P. furiosus* ferredoxin has an OH^- ligand, and that this can be displaced by OD^- (D_2O) in the $S = \frac{1}{2}$ state of the cluster, but not in the $S = \frac{3}{2}$ form. Thus there are questions: would the unique Fe site of the [4Fe–4S] cluster (which we will now refer to as Fe_a) bind other ligands by displacing OH^-, and do the two spin states of the cluster show different reactivities? Cyanide is again the ligand of choice, as this is a potent inhibitor of many Fe–S-containing enzymes, as well as a substrate of nitrogenase. As shown in Fig. 11 (*127*) cyanide has a dramatic effect on the EPR properties of the $[4Fe–4S]^{1+}$ cluster of *P. furiosus* ferredoxin. Incubation of the reduced protein with a 250-fold excess of cyanide for 2 hr (pH 7.5–10.5) results in the complete conversion of the EPR resonances from both the $S = \frac{1}{2}$ and $S = \frac{3}{2}$ forms to a new $S = \frac{1}{2}$ resonance, $g = 2.09$, 1.95, and 1.92 (*127*). The latter represents 1 spin/mole, and can still be seen at 60 K, which is in contrast to the EPR absorption from the native cluster, as this is observed only below 15 K. Substantial broadening is observed using the ^{57}Fe-enriched protein (Fig. 11c), showing that the EPR signal induced by cyanide does arise from an Fe-containing center. However, its EPR properties are unlike those of any other biological 4Fe center; indeed, they are more reminiscent of reduced ferredoxin-type 2Fe clusters.

Evidence for the binding of cyanide to only Fe_a and without destruction or rearrangement of the $[4Fe–4S]^{1+}$ cluster is provided by the following. First, cyanide showed no reaction with the 4Fe clusters of *C. pasteurianum* ferredoxin (which have complete cysteinyl coordination) nor with the 3Fe form of *P. furiosus* ferredoxin (which lacks Fe_a). Second, the MCD of the cyanide-treated protein was characteristic of $S = \frac{1}{2}$ 4Fe-type rather than 2Fe-type centers. Third, simply removing the cyanide completely regenerates the characteristic $S = \frac{1}{2}$ and $S = \frac{3}{2}$ resonances of native protein. Fourth, as described above, the ferre-

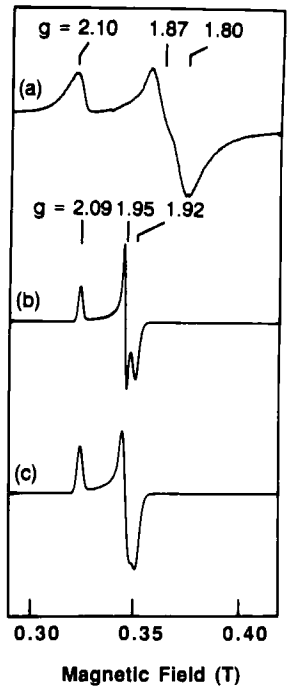

FIG. 11. EPR spectra of the cyanide-treated ferredoxin from *P. furiosus*. (a) Reduced ferredoxin (6 mg/ml); (b) after the addition of a 250-fold excess of potassium cyanide; (c) ^{57}Fe-reconstituted ferredoxin after cyanide treatment. The spectra were recorded at 20 K using 1-mW microwave power. Taken from Ref. *127*.

doxin is exceptionally resistant to denaturation, therefore, the cyanide effect is unlikely to arise from cyanide-induced conformational changes of the protein. Fifth, anaerobic oxidation of the cyanide-treated protein by thionine generates the 3Fe form, indicating loss of Fe_a from an intact 4Fe cluster (*127*). Presumably, this is related to the fact that ferricyanide, and not other high potential oxidants such as thionine or 2,6-dichlorophenolindophenol, can effectively remove a single Fe atom from [4Fe–4S] clusters. Sixth, preliminary data indicate that a ^{13}C ENDOR resonance is observed from the ^{13}CN-treated protein (C. Fan, R. Conover, J.-B. Park, M. W. W. Adams, M. K. Johnson, and B. M. Hoffman, unpublished, 1991). These results therefore provide the first evidence for exogenous ligand binding to a noncysteinyl-ligated Fe atom of a $[4Fe–4S]^{1+}$ cluster in a bacterial ferredoxin (*127*). In contrast to the binding of OH^-/OD^-, cyanide reacts with the $S = \frac{3}{2}$ form of the

4Fe cluster in *P. furiosus* ferredoxin. Preliminary results using lower cyanide concentrations indicate that cyanide preferentially reacts with the $S = \frac{1}{2}$ ground state, but as yet conditions for exclusive reactivity have not been obtained.

The presence of a noncysteinyl ligand to one Fe atom (Fe_a) of the [4Fe–4S] cluster in *P. furiosus* ferredoxin therefore has very useful consequences. These are discussed with reference to Fig. 8. Fe_a is able to bind exogenous ligands, such as OD^- and cyanide, and because of the reactivity of Fe_a, its removal is greatly facilitated (by ferricyanide). When cyanide is bound, facile removal of Fe_a occurs upon oxidation. The binding of ligands to Fe_a appears to be directly analogous to the reaction of the catalytic Fe–S center in aconitase with its substrates, and possibly to the reactions catalyzed by enzymes such as hydrogenase and nitrogenase. Moreover, the degree of reactivity of Fe_a seems to be related to the spin state ($S = \frac{1}{2}$ or $S = \frac{3}{2}$) of the cluster. In addition, replacement of Fe_a with other metal ions readily takes place, presumably because of the absence of the reactive thiol of the substituted cysteinyl residue. In fact, our preliminary experiments indicate that Co^{2+} or Zn^{2+} are incorporated into the 3Fe center even more readily than Ni^{2+}. It is assumed in Fig. 8 that OH^- binds to the M site. Although there is no direct evidence for this, the M site appears to bind ligands (cyanide) in the same fashion as Fe_a. Indeed, we have recently shown that cyanide dramatically changes the EPR and MCD properties of the Zn and Co clusters (R. C. Conover, M. Finnegan, J.-B. Park, M. W. W. Adams, and M. K. Johnson, unpublished, 1991). In other words, exogenous ligands such as cyanide appear to interact only with the unique, noncysteinyl and exchangeable metal site of the cubane cluster of *P. furiosus* ferredoxin, whether the metal be Fe, Zn, Ni, or Co. Although it remains to be seen if Fe–S-containing enzymes such as CO dehydrogenase (where M = Ni), nitrogenase (where M = Mo, V, or Fe), and Fe hydrogenase (where M = Fe) utilize the reactivity of such cubane clusters, further studies of the properties of this structure in *P. furiosus* ferredoxin should yield useful information on the chemical diversity of the [M–3Fe–4S] unit in an extremely stable biological environment.

C. Rubredoxin (Fe)

Rubredoxins are a class of bacterial electron transfer proteins that contain a single iron atom coordinated by the sulfur atoms of four cysteinyl residues (*128*). All are monomeric proteins of molecular weight approximately 6000. The complete amino acid sequences of 11

rubredoxins are known (*129–140*) and four crystal structures have been reported (*141, 142*). As the simplest known class of redox protein, comparative studies of rubredoxins isolated from divergent species have the potential to provide insight into both the minimum structural requirements for this protein and the residues that influence electron transfer and the redox properties of the iron site, as well as phylogenetic relationships. In addition, the study of thermostable rubredoxins could provide information on the mechanisms of stabilizing proteins at extreme temperatures. To date, the only structural information available on rubredoxins comes from those purified from eubacteria, and all but one of them are from mesophilic species, the exception being *Clostridium thermosaccharolyticum* (*131*), which grows optimally at 55°C. *Pyrococcus furiosus* rubredoxin is the first to be purified from a hyperthermophilic bacterium, and also the first from an archaebacterium.

The molecular properties of *P. furiosus* rubredoxin are similar to those of the mesophilic proteins (*144*). Its molecular weight, estimated by gel filtration, was 6800 ± 1000, which is in reasonable agreement with the value calculated (5397; see below) from the amino acid sequence. The UV-visible spectrum of the oxidized protein is also typical of other rubredoxins: the absorption coefficients at the maxima are 25.6 (280 nm), 10.7 (390 nm), and 9.22 (494 nm) $mM^{-1}\ cm^{-1}$, and the A_{494}/A_{280} ratio is 0.36. In accordance, the protein contains 1.2 ± 0.2 g-atoms of Fe/5282 g of protein, but no acid-labile sulfide (*144*). Oxidized *P. furiosus* rubredoxin also exhibits the characteristic rubredoxin EPR spectrum (g = 4.3 and 9.4), which arises from the high-spin Fe(III) site. The midpoint potential of the Fe site at 25°C and pH 8.0 is 0 ± 15 mV (J.-B. Park and M. W. W. Adams, unpublished data, 1991). The effect on the E_m value of *P. furiosus* rubredoxin of temperature and of increasing the pH to 10 is shown in Fig. 12. Surprisingly, the E_m value at pH 10 is approximately 60 mV lower than that at pH 8.0 (at 25°C), suggesting that an ionizable protein residue has a direct influence on the redox properties of the Fe site (see, for example, Ref. *145*). Whether this effect is unique to the *P. furiosus* protein is not known, as the pH dependence of the E_m value of a mesophilic rubredoxin has not been reported. Only a slight decrease (~0.3 mV/°C) in the E_m value is seen at both pH values upon raising the temperature to 50°C, but between 50 and 90°C, rather dramatic changes are observed. The E_m value decreases fairly linearly by 2.7 mV/°C at pH 10.0, and by 3.5 mV/°C at pH 8.0. These changes are greater than those found with *P. furiosus* ferredoxin (−1.7 mV/°C, 20–80°C; Section III,B,1) and with *P. furiosus* aldehyde ferredoxin oxidoreductase (~ −2.0 mV/°C, 20–70°C; Section III,D). All of these values are greater than those reported for the mesophilic redox protein, cytochrome *c* (−0.5 to −1.4 mV/°C, 5–60°C; Ref.

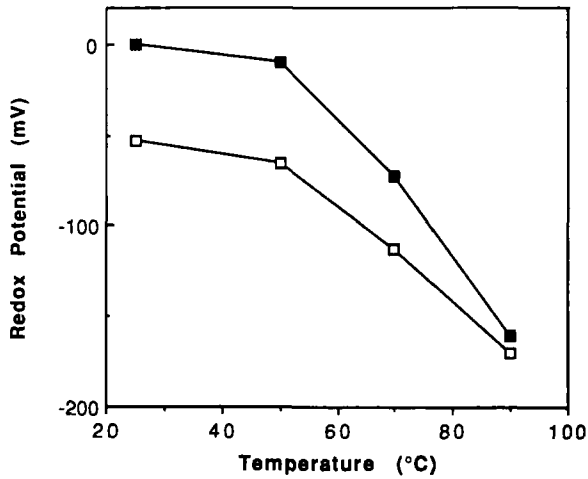

FIG. 12. The effect of temperature and pH on the midpoint potential of rubredoxin from *P. furiosus*. Redox titrations were monitored using EPR spectroscopy and were carried out at pH 8.0 (closed symbols) or 10.0 (open symbols) at the indicated temperature (J. B. Park and M. W. W. Adams, unpublished data, 1991).

146). In addition, the E_m value of *P. furiosus* rubredoxin showed a transition at 50°C, while *P. furiosus* ferredoxin showed a sharp transition at 80°C and a temperature-dependent transition was not evident for the aldehyde ferredoxin oxidoreductase (Section III,D). Each of these proteins therefore has a different dependence on temperature, indicating that the temperature-dependent data are not an electrode artifact or due to pH changes, and it is assumed that they reflect the actual E_m value of a redox center at a particular temperature. At 100°C, the optimum growth temperature for *P. furiosus*, the redox potential of the rubredoxin is estimated at approximately −200 mV (Fig. 12).

As might be expected, *P. furiosus* rubredoxin is considerably more thermostable than its mesophilic counterparts. For example, the UV-visible and EPR properties of the protein (1.0 mg/ml in 50 m*M* EPPS buffer, pH 8.4) are unaffected after a 24-hr incubation at 95°C. For comparison, the rubredoxin from *C. pasteurianum* is rapidly denatured at 80°C (*147*), whereas the protein from *D. gigas* loses 50% of its visible absorption ($t_{50\%}$) after approximately 2 hr at 80°C (*148*). The rubredoxin from the moderately thermophilic sulfate-reducing bacterium, *Thermodesulfobacterium commune*, which grows optimally at 70°C, is slightly more stable, having a $t_{50\%}$ value of about 6 hr at 80°C (*148*). Unfortunately, there is little indication of the mechanisms responsible

for the enhanced thermostability of the *P. furiosus* protein from its amino acid sequence. For example, the sequence of *P. furiosus* rubredoxin (*144*) is aligned with those of the rubredoxins from mesophilic organisms (Fig. 13). The overall sequence homology (identity) of *P. furiosus* rubredoxin with the others ranges from 42 to 67%, which is similar to the homologies (41–90%) found between the mesophilic rubredoxins. A previous study (*131*) of the amino acid sequences of 10 mesophilic rubredoxins noted 15 conserved residues. As indicated in Fig. 13, 14 of these residues, which include the four cysteinyl residues that bind the Fe atom together with an adjacent prolyl residue, are also conserved in *P. furiosus* rubredoxin. The exception, which may be of some significance (see below), is the N-terminal methionine residue. In addition, four unique residues previously identified in the rubredoxin of the moderate thermophile, *C. thermosaccharolyticum,* might confer stability to this protein (*131*). Of these, though, only one (Trp 4) is present in the *P. furiosus* protein. Also indicated in Fig. 13 are the seven residues that are present in *P. furiosus* rubredoxin but not in any of the others (excluding the absence of the N-terminal methionine).

The complete amino acid sequence of only one hyperthermophilic enzyme is known—that of glyceraldehyde-3-phosphate dehydrogenase (GAPD) from *Pyrococcus woesii* (*149*). Compared to mesophilic GAPDs, this shows a striking preference for phenylalanine and discrimination against aspartate, methionine, and cysteine (*149*). However, similar characteristics are not evident when one compares the sequence of the hyperthermophilic *P. furiosus* rubredoxin with the others listed in Fig. 13. Indeed, systematic comparisons show no obvious preference for any amino acid in *P. furiosus* rubredoxin compared with the others listed in Fig. 13. Perhaps the exception is isoleucine (four residues in *P. furiosus* rubredoxin, three in the *C. thermosaccharolyticum* protein, and two or less in the others), but the significance of this is hard to rationalize. Obviously, three-dimensional structures rather than amino acid sequence comparisons are required to determine the differences in protein structures that result in mesophilic rubredoxins rapidly denaturing at 80°C and *P. furiosus* rubredoxin being stable for 24 hr at 95°C.

NMR provides a particularly powerful approach to investigate the structural properties of low-molecular-weight proteins such as rubredoxins. Unfortunately, one- and two-dimensional ^{1}H NMR of the oxidized and reduced *P. furiosus* protein showed substantial paramagnetic line broadening, and this prevented a detailed structural study of the native protein. High-quality spectra were obtained though for the Zn-substituted protein (*144*). In addition, the intensities and the chemi-

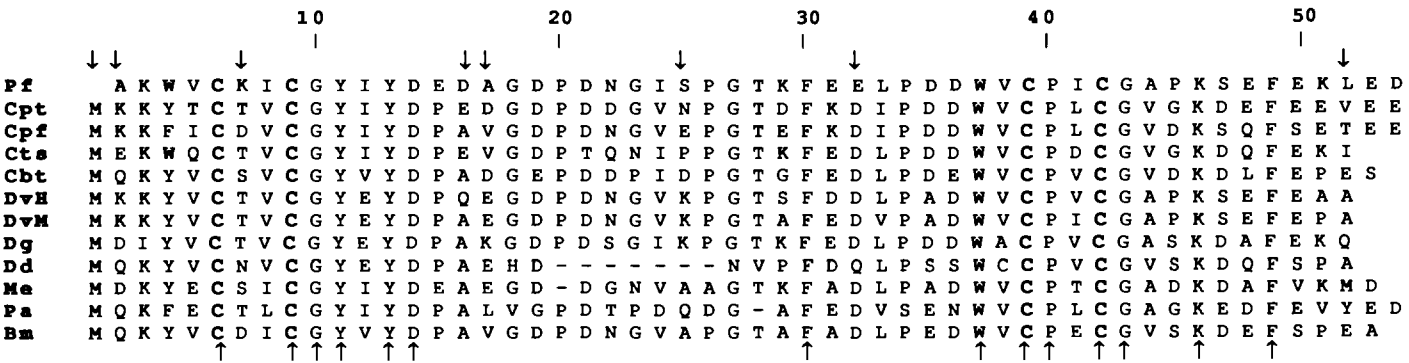

FIG. 13. A comparison of the amino acid sequence of the rubredoxin from *P. furiosus* and those from anaerobic eubacteria. Abbreviations and sources of the data: Pf, *Pyrococcus furiosus* (*144*); Cpt, *Clostridium pasteurianum* (*128, 129*); Cpf, *Clostridium perfringens* (*130*); Cts, *Clostridium thermosaccharolyticum* (*131*); Cbt, *Chlorobium thiosulfatophilum* (*132*); DvH, *Desulfovibrio vulgaris* strain Hildenborough (*133, 134*); DvM, *Desulfovibrio vulgaris* strain Miyazaki (*135*); Dg, *Desulfovibrio gigas* (*136*); Dd, *Desulfovibrio desulfuricans* (*137*); Me, *Megasphaera elsdenii* (*138*); Pa, *Peptococcus aerogenes* (*139*); Bm, *Butyribacterium methylotrophicum* (*140*). Conserved cysteines are given in boldface letters; ↓ indicates residues (or lack of) unique to *P. furiosus* rubredoxin and ↑ indicates residues conserved in all known rubredoxins.

cal shifts of the cross-peaks in the two-dimensional NOESY (nuclear Overhauser effect) data that could be observed from the native protein matched those in the spectrum from the Zn protein, suggesting that Fe replacement by Zn produced minimal structural changes at the metal-binding site. This was expected since the backbone conformation of C-X-X-C-G sequence in the Zn domain of retroviral zinc finger proteins is virtually identical to the structure of the analogous residues in the Fe domain in mesophilic rubredoxins (*150*). Moreover, the preliminary NMR data of the Zn rubredoxin showed that its secondary structure is essentially the same as that of the rubredoxin from the mesophile, *C. pasteurianum*. These proteins have 60% sequence identity. Thus, both of these rubredoxins contain a similarly packed hydrophobic core, and a three-stranded antiparallel β sheet with several tight turns. Although the determination of the complete three-dimensional structure of *P. furiosus* rubredoxin is still underway, one potentially significant finding concerns the N terminus of the protein. As shown in Fig. 13, in contrast to all the other rubredoxins, the *P. furiosus* protein lacks an N-terminal methionine residue. The NMR data from *P. furiosus* Zn rubredoxin clearly show (*144*) that Ala 2 (which is the N terminus in the numbering system of Fig. 13) is part of the β sheet and its amino group interacts with the carboxyl groups of Glu 15 and Glu 53. Since, with one exception, the mesophilic rubredoxins have Pro at position 15, and all of them have an N-terminal methionine, the *P. furiosus* protein is uniquely able to generate such interactions. These may significantly stabilize one end of the β sheet and prevent its "unraveling" at extreme temperatures. Such an effect should be observed in variable high-temperature NMR studies of the *P. furiosus* protein, and these are in progress.

Finally, a word on the physiological role of rubredoxin in *P. furiosus*. Mesophilic rubredoxins have been suggested to function as electron carriers in the primary metabolic pathways of such diverse organisms as acetogenic (*151, 152*), methylotrophic (*153*), sulfate-reducing (*135, 154*), and nitrate-reducing (*130*) bacteria. On the other hand, a role for this protein has yet to be postulated in saccharolytic organisms, such as *C. pasteurianum, C. thermosaccharolyticum,* and *Megasphaera elsdenii*. This is of some relevance, since *P. furiosus* appears to grow by the fermentation of certain simple and complex carbohydrates to organic acids, CO_2, and H_2 (Ref. *19*; see Section III,E). However, it is somewhat curious that the rubredoxins that have been purified are a remarkably homologous group of proteins, especially considering the range of metabolisms exhibited by the bacteria listed in Fig. 13. Moreover, they all have E_m values near 0 mV (at ambient temperature), and for the various

electron acceptor roles that have been suggested for this protein, it is far from clear what oxidizes reduced rubredoxin. Furthermore, in widely divergent species such as *P. furiosus* (a hyperthermophilic archaebacterium) and, for example, *C. pasteurianum* (a mesophilic eubacterium), both of which are obligately dependent on the reduction of protons to H_2 for growth (E_m = −420 mV, 25°C), the role or even necessity of a rubredoxin (E_m ~ 0 mV, 25°C) is hard to rationalize. It may therefore be hypothesized that rubredoxin has the same physiological role in all of the anaerobic organisms listed in Fig. 13: that is, the fact that this protein is redox active may be merely fortuitous. For example, rubredoxin may be a storage form of Fe(II) with complete S ligation that is readily available for Fe–S cluster synthesis, or it may be a sensor of the availability of Fe(II) and play some regulatory role in anaerobic organisms. As yet, however, there is no evidence for these suggestions, although it should be mentioned that a ferredoxin has been postulated to regulate gene expression in response to cellular Fe(II) concentrations in the aerobic bacterium, *Azotobacter vinelandii* (*155*). In any event, the role of rubredoxin in *P. furiosus* is at present a mystery.

D. Aldehyde Ferredoxin Oxidoreductase (W–Fe–S)

During our preliminary growth studies of *P. furiosus* it was found that the addition to the growth medium of W (in the form of tungstate) significantly stimulated cell growth (*31*). A red-colored, W-containing protein, abbreviated RTP for "red tungsten protein," was subsequently identified during the purification of *P. furiosus* hydrogenase and was purified under strictly anaerobic conditions to homogeneity (*156*). RTP is a monomeric protein of M_r 85,000 and contains approximately 1W, 7Fe, and $5S^{2-}$ atoms/mole. W is an element seldom used in biological systems; indeed, only one W-containing enzyme was previously known—a formate dehydrogenase purified from the acetogen, *C. thermoaceticum*, by Ljungdahl and co-workers (*157*). However, *P. furiosus* RTP did not catalyze the oxidation of formate. Thus, there were obvious questions: what is the nature of the Fe and W in RTP, and what reaction does it catalyze? The following discussion shows how at least partial answers to these questions came from studies using electrochemistry and EPR spectroscopy.

RTP as isolated in dithionite-containing buffer has absorption throughout the visible region of the spectrum (Σ_{425} = 8800 M^{-1} cm^{-1}), with a broad feature near 540 nm (*156*). The protein turns green-brown in color when it is exposed to air or oxidized by ferricyanide. This is

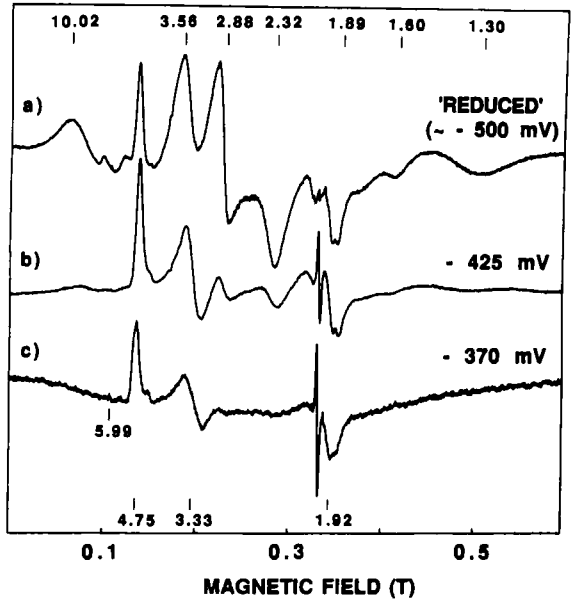

FIG. 14. EPR spectra of the red tungsten protein (RTP) of *P. furiosus*. The sample contained RTP (14 mg/ml) in 50 m*M* Tris/HCl buffer, pH 8.0, containing sodium dithionite (a) or poised at the indicated potential (b and c). The spectra were recorded at 6 K using 100-mW microwave power. The sharp isotropic signal at $g = 2$ in spectra b and c originates from redox mediators. Taken from Ref. *156*.

accompanied by the loss of the 540-nm absorption and a large increase in the absorption near 400 nm ($\Sigma_{425} = 17{,}600\ M^{-1}\ cm^{-1}$). Titrations show that the ferricyanide-oxidized protein is reduced by the equivalent of approximately 1.5 electrons/mole using sodium dithionite as the reductant (pH 8, 25°C), indicating that the protein contains two redox-active centers that are not completely reduced by sodium dithionite. The dithionite-reduced protein exhibits a remarkable EPR spectrum with g values ranging from 10.0 to 1.3 (Fig. 14), unlike that of any other biological or synthetic Fe–S system. The thionine-oxidized protein is EPR silent. Upon partial oxidation (to -370 mV, pH 8) of the dithionite-reduced protein (~ -500 mV), EPR from a single paramagnetic species with $S > \frac{1}{2}$ is observed (Fig. 14). These resonances can be interpreted using a spin Hamiltonian with an isotropic Zeeman interaction. For example, with $E/D = 0.135, D > 0$, and $g_0 = 2$, the $S = \frac{3}{2}$ spin Hamiltonian predicts $g(x, y, z) = 3.13, 4.75$, and 1.89 for the ground state doublet, values that are in reasonable agreement with the observed g

values of 3.33, 4.75, and 1.92. Theory also predicts $g(x, y, z) = 0.84$, 0.74, and 5.90 for the upper doublet. A minor resonance is observed at $g = 5.99$, and this is assigned to the excited doublet as its intensity increases with increasing temperature ($\leq$10 K). Analysis of the temperature dependence of the intensity ratio of the $g = 4.75$ (lower) and $g = 5.99$ (upper) resonances indicated that $D = 4.3 \pm 0.5$ cm^{-1} (*156*).

One of the redox centers in RTP, which will be termed center A, therefore has a well-defined $S = \frac{3}{2}$ ground state. So, how does the complex spectrum of the dithionite-reduced protein arise? As shown in Fig. 14, upon reduction of partially oxidized RTP, the intensity of the EPR signal from reduced center A (A_{red}) *increases* in intensity before decreasing to that seen in the reduced sample. This suggests that the complex spectrum of the reduced protein is a result of the spin–spin interaction of A_{red} with a second but nonidentical paramagnetic species (center B). Center B has a slightly lower E_m value than center A, so that upon reduction of the oxidized protein, the spectrum of A_{red} is observed first. The EPR spectrum of B_{red} is not seen because as soon as this center is reduced, it interacts with A_{red} to give a complex EPR spectrum of the spin-coupled system. This spectrum dominates the EPR absorption of the dithionite-reduced protein, but this redox state of RTP also exhibits the EPR spectrum of the remaining A_{red}, i.e., that which is not interacting with B_{red}, as evidenced by the $g = 4.75$ resonance. Center A and the resultant spin-coupled system can therefore be differentiated potentiometrically. As will now be described, this enables the redox properties of center B to be evaluated, in spite of the fact that its EPR spectrum is not apparent.

The relative amounts of the oxidized and reduced forms of redox centers A and B can be calculated at a given potential using the Nernst equation [Eq. (1)], where n is the number of electron transfers (see, for example, Refs. *158* and *159*). This simplifies to Eq. (2) for a one-electron

$$E_h = E_m + \frac{RT}{nF} \ln \frac{[\text{oxidized}]}{[\text{reduced}]} \tag{1}$$

$$E_h = E_m + 58.1 \log \frac{[\text{oxidized}]}{[\text{reduced}]} \tag{2}$$

transfer at 20°C (note that in temperature-dependent studies, the temperature term in the Nernst equation affects only the slope of the redox curve). The fractions of the centers in their reduced forms ($F_{A_{red}}$ and $F_{B_{red}}$) when the protein (P) is at a potential of E_h can be calculated by Eqs. (4) and (5), where E_{mA} and E_{mB} are their respective

$$F_{A_{red}} = [10^{(E_h - E_{mA})/y} + 1]^{-1} \tag{4}$$

$$F_{B_{red}} = [10^{(E_h - E_{mB})/y} + 1]^{-1} \quad (5)$$

midpoint potentials (see Ref. *160*). Let the fraction of the protein in the oxidized state, i.e., with neither center reduced, be P^0, that with only one of the two centers reduced be P^-, and that with both reduced be P^{2-}. The fractions of the total protein in these two redox states at a given potential can be calculated by Eqs. (6) and (7). The singly reduced

$$[P^0] = (1 - F_{A_{red}})(1 - F_{B_{red}}) \quad (6)$$

$$[P^{2-}] = F_{A_{red}} F_{B_{red}} \quad (7)$$

protein (P^-) can exist in two different redox states, where each has only one of the two centers reduced ($A_{red} \cdot B_{ox}$ and $A_{ox} \cdot B_{red}$). Let the fraction of the protein that has only center A reduced be P_A^- ($A_{red} \cdot B_{ox}$), and that with only center B reduced be P_B^- ($A_{ox} \cdot B_{red}$). Equations (8) and (9) show how their concentrations may be determined.

$$[P_A^-] = 1 - (F_{A_{red}} F_{B_{red}}) - (1 - F_{A_{red}}) = F_{A_{red}}(1 - F_{B_{red}}) \quad (8)$$

$$[P_B^-] = 1 - (F_{A_{red}} F_{B_{red}}) - (1 - F_{B_{red}}) = F_{B_{red}}(1 - F_{A_{red}}) \quad (9)$$

With *P. furiosus* RTP, the concentration $[P^{2-}]$ of the doubly reduced protein can be measured by the amplitude of the $g = 2.88$ EPR signal (Fig. 14), whereas the fraction of the protein with only center A reduced, $[P_A^-]$, is proportional to the intensity of the $g = 4.75$ resonance. Figure 15 shows the results of a redox titration performed at 20°C and pH 8.0. The theoretical plots are calculated using E_m values for center A and center B of −410 mV and −500 mV, respectively. The data clearly correspond to the predicted redox behavior for two interacting centers, with the intensity of the $g = 4.75$ resonance rising and falling as the potential decreases. This type of theoretical analysis predicts that a maximum of only 2.1% of the protein has only center B reduced (at −455 mV), hence, it is unlikely that its EPR signal would be observed. Figure 15 also shows that the apparent E_m value (at pH 8.0) of the doubly reduced protein ($A_{red} \cdot B_{red}$) is −505 mV, and at this potential most of the remaining protein has only center A reduced (47%). Thus, at the potential usually obtained using sodium dithionite as the reductant (~−500 mV at pH 8.0), the protein is reduced by 1.5 electrons/mole, in agreement with the visible absorption data described above (*156*). The effective reducing potential of sodium dithionite decreases with increasing pH (*161*) so that at pH 9.0 the protein is reduced to a greater extent than it is at pH 8.0 (Fig. 15). However, the E_m values of center

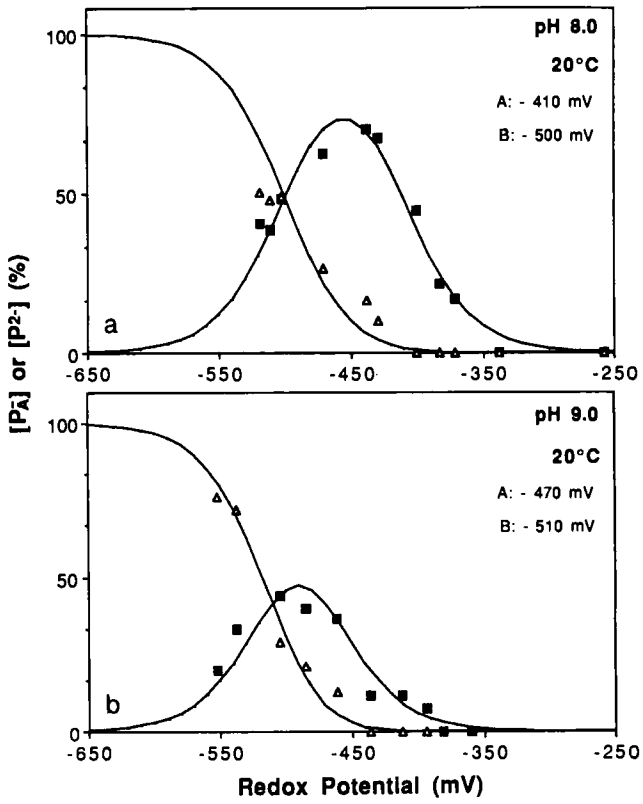

FIG. 15. Determination of the redox behavior of center A and center B in the red tungsten protein (RTP) of *P. furiosus*. Redox titrations of RTP were carried out at 20°C at pH 8.0 (a) and pH 9.0 (b). $[P^{2-}]$ (open triangles) is the concentration of the doubly reduced protein ($A_{red} \cdot B_{red}$) as measured by the amplitude of the $g = 2.88$ signal shown in Fig. 14. $[P_A^-]$ (closed squares) is the concentration of the protein with only center A reduced ($A_{red} \cdot B_{ox}$) as measured by the amplitude of the $g = 4.75$ resonance (Fig. 14). The theoretical curves were calculated as described in the text using the indicated E_m values for the two redox centers. Modified from Ref. *156*.

A and center B also decrease with increasing pH (>8.0), so the protein cannot be fully reduced with sodium dithionite even at pH 10. Such a pH dependence also indicates that a proton is involved in the reduction and oxidation of each center. In addition, the E_m values of centers A and B decrease with increasing temperature ($\Delta E_m/\Delta T \sim -2$ mV/°C at pH 8.0 for both centers). At 100°C, the optimum growth temperature of *P. furiosus*, the E_m values are estimated at -590 mV (A) and -650

mV (B), values that are more than 150 mV lower than those determined at ambient temperature (*156*).

Analyses using visible absorption spectroscopy show that reduced RTP transfers electrons to *P. furiosus* ferredoxin ($E_m \leq -550$ mV at 100°C) but not to NAD(P) (*156*). It was therefore postulated (*156*) that RTP catalyzes an oxidoreductase-type reaction of extremely low potential (≤ -500 mV), in which the mechanism involves the transfer of two protons and two electrons, and ferredoxin serves as the electron donor. The problem is that few biochemical reactions take place at such low potentials, and RTP did not catalyze the oxidation of obvious substrates such as (the potentials are quoted at 20°C, pH 7, taken from Ref. *162*) CO (to CO_2, $E_m = -510$ mV), pyruvate (to acetyl-CoA, $E_m = -520$ mV), or 2-ketoglutarate (to succinyl-CoA, $E_m = -520$ mV). However, RTP does catalyze a rather unusual reaction: the oxidation of aldehydes to the corresponding acid [Eq. (10)]. The aldehyde/acid redox couple has a midpoint of around -560 mV (*163*), so this reaction is consistent with the conclusions from the spectroscopic analyses. RTP is therefore now termed aldehyde ferredoxin oxidoreductase, or AOR (*164*). The likely physiological substrate for AOR is discussed in Section III,E.

$$RCHO + H_2O = RCOOH + 2H^+ + 2e^- \quad (10)$$

We now turn to the nature of the redox centers in AOR and the source of the novel EPR signals shown in Fig. 14. The striking similarity of the EPR properties of reduced center A to those of synthetic [W–3Fe–4S] and [Mo–3Fe–4S] clusters (*91, 126*), all of which have $S = \frac{3}{2}$ ground states, led to the proposal that center A might be a [W–3Fe–4S] cluster (*156*). However, a recent study of dithionite-reduced AOR by extended X-ray absorption fine structure (EXAFS) spectroscopy (*165*) showed that this is not the case: no W–Fe interactions were observed in the W L_{III} edge EXAFS. AOR therefore contains a monomeric W site. The best fits for the data were obtained using two W=O at 1.74 Å, three W—S at 2.41 Å, and one W—O/N at 2.16 Å. The presence of the two oxo ligands and nature of the absorption edge spectrum showed that the W is present as W(VI), even though the sample contained sodium dithionite (*165*). The potential of the W(VI)/W(V) couple is therefore likely to be much less than -500 mV (at 25°C), which would be consistent with the aldehyde/acid redox couple. A mononuclear Mo(VI) center has been identified in a variety of molybdenum enzymes, in which it is bound to a pterin cofactor (see Refs. *166* and *167* and references therein). Indeed, the number and distances of the ligands to the Mo in, for example, sulfite oxidase (*168*), one of the best studied of the molybdopterin enzymes, are virtually identical to

those just described for W in AOR. Moreover, fluorescence spectroscopy of AOR after acid treatment shows that it contains a pterin-type cofactor that is similar, although not identical, to molybdopterin (*164*). A proposed structure of the W site in AOR is given in Fig. 16. By analogy with the molybdopterin-containing enzymes, the W site in AOR is probably reduced to the V and IV states during the catalytic cycle. It should therefore be possible to induce a transient W(V) EPR signal from AOR upon treatment with substrates. Since AOR is unaffected by a 6-hr incubation at 80°C, is virtually inactive at ambient temperature, and the optimum temperature for catalytic activity is ≥95°C (*164*), it is well suited for the isolation of transient intermediates. Such "cryoenzymological" studies at 4–20°C, which approach 100°C below the optimum temperature for both catalysis and cell growth, are underway.

Since the III and V valence states of W are paramagnetic, the identification of a mononuclear W(VI) site in dithionite-reduced AOR rules out the possibility of W contributing to the EPR absorption. The EPR spectra shown in Fig. 14 must therefore arise from Fe–S centers. Several biological $[4Fe–4S]^{1+}$ clusters, including that in *P. furiosus* ferredoxin, are now known to exist in an $S = \frac{3}{2}$ spin state (although all are as mixtures of $S = \frac{1}{2}$ and $S = \frac{3}{2}$; see Section III,2,a,1). Considering the metal content of AOR (~7 Fe atoms/mole), it is not unreasonable to suggest that center A ($S = \frac{3}{2}$) is a $[4Fe–4S]^{1+}$ cluster. This would be the first example of a biological 4Fe cluster with a ground state spin of exclusively $S = \frac{3}{2}$. As for center B in AOR, the EPR analyses show only that it is paramagnetic in the reduced state ($S \geq \frac{1}{2}$), and the Fe content of the enzyme is consistent with it being either a 2Fe- or a 4Fe-type center. However, preliminary data from resonance Raman indicate that AOR contains only 4Fe-type centers (W. Fu and M. K. Johnson, unpublished data, 1991). The unusual EPR properties of reduced AOR are therefore proposed to arise from two spin-coupled 4Fe centers, one $S = \frac{3}{2}$ and one $S \geq \frac{1}{2}$, that have different midpoint potentials. As shown

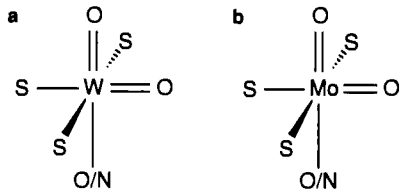

FIG. 16. Proposed structure of (a) the W site in dithionite-reduced aldehyde ferredoxin oxidoreductase of *P. furiosus* (*165*) and (b) the Mo site in oxidized mammalian sulfite oxidase (*168*).

in Fig. 17, these are proposed to mediate electron transfer between the tungstopterin-containing catalytic site of AOR and ferredoxin, the physiological electron carrier for the enzyme.

Pyrococcus furiosus AOR is therefore a unique type of Fe–S-containing enzyme, although some fundamental properties of its Fe–S clusters, such as the spin state and EPR spectrum of center B, are not known at present. AOR is also the first aldehyde-oxidizing enzyme to be isolated from any archaebacterium or any extreme thermophile, and is the first CoA-independent aldehyde oxidoreductase from a nonacetogenic anaerobe.

E. Role of Fe–S Proteins in H_2 Production

Pyrococcus furiosus AOR catalyzes the oxidation of a wide range of aldehydes, e.g., acetaldehyde, propionaldehyde, crotonaldehyde and glyceraldehyde, to the corresponding acid, using either methyl viologen or *P. furiosus* ferredoxin, but not NAD(P), as the electron acceptor. It does not oxidize glucose, glyoxylate, or glyceraldehyde-3-phosphate (*164*). So, why does *P. furiosus* need an enzyme that oxidizes aldehydes, and need it at very high cellular concentrations (at least five times that of the hydrogenase)? The organism obtains energy for growth by the fermentation of carbohydrates to organic acids, CO_2, and H_2. One would expect the organism to use the Embden–Meyerhof pathway for converting glucose ultimately to acetate, as do saccharolytic, anaerobic eubacteria (*162*). However, this pathway does not require an enzyme that oxidizes aldehydes, and the activities of key enzymes such as glyceraldehyde-3-phosphate dehydrogenase and phosphoglycerate ki-

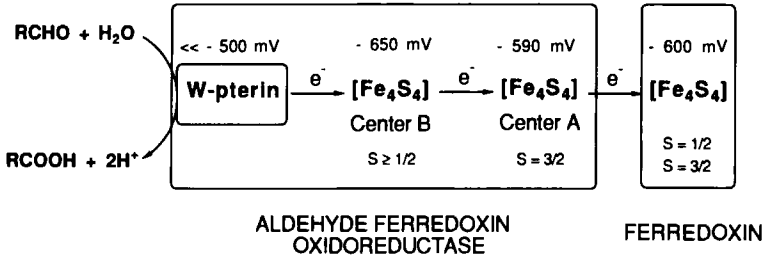

FIG. 17. Proposed redox centers and pathway of electron transfer at 100°C during aldehyde oxidation by aldehyde ferredoxin oxidoreductase of *P. furiosus*. The spin states of the 4Fe clusters in aldehyde ferredoxin oxidoreductase and ferredoxin and the redox potentials of all redox centers (estimated at 100°C) are indicated.

nase are present in *P. furiosus* at relatively low levels (*164*). We therefore proposed (*164*) that *P. furiosus* has a novel pathway for oxidizing glucose. It is analogous to the NAD(P)-dependent pathway thought to occur in some aerobic archaebacteria (*169–171*), but differs in that all the oxidation steps needed to convert glucose to acetate are catalyzed by ferredoxin-linked oxidoreductases. As shown in Fig. 18, AOR is

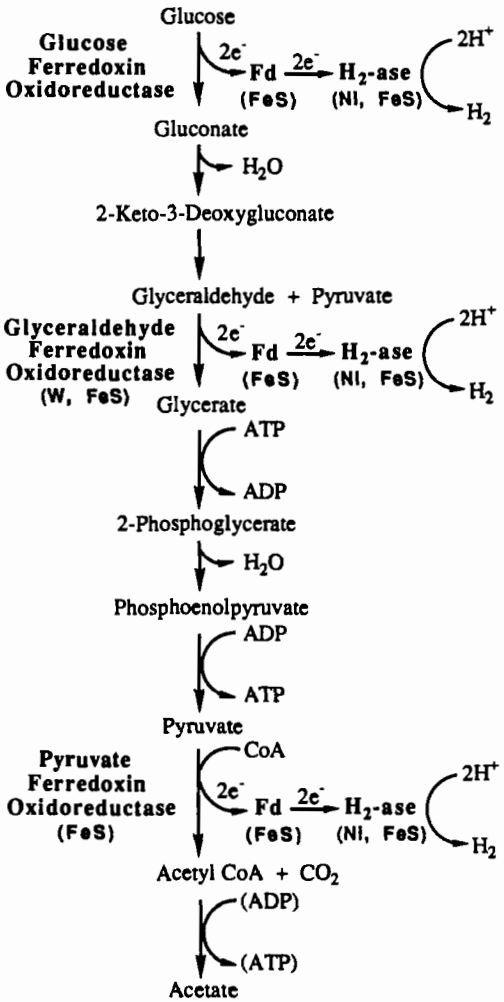

FIG. 18. Proposed "pyroglycolytic" pathway in *P. furiosus* and the role of Fe–S-containing proteins. Modified from Ref. *164*.

proposed to catalyze a key step in the "pyroglycolytic" pathway—it functions as a glyceraldehyde ferredoxin oxidoreductase and converts glyceraldehyde to glycerate. The first step in the pathway is catalyzed by another new enzyme, glucose ferredoxin oxidoreductase (GOR), which generates gluconate from glucose. The final oxidation step is catalyzed by a more conventional pyruvate ferredoxin oxidoreductase (POR), yielding acetyl-CoA. Since ferredoxin is the physiological electron donor for *P. furiosus* hydrogenase, its use as an electron acceptor for each of these oxidoreductases enables the reductant generated from glucose oxidation to be directly removed as H_2, via the hydrogenase.

A unique consequence of the proposed pyroglycolytic pathway for H_2 production is that *P. furiosus* could generate acetyl-CoA from glucose without the participation of NAD(P)H. These cofactors are particularly thermolabile (*172*), and their replacement in a primary metabolic pathway by a thermostable ferredoxin may be one of the key adaptations that enables this organism to grow at temperatures in excess of 100°C. In addition, the proposed pathway may not be limited to *P. furiosus*. We have found that the growth of two other heterotrophic and extremely thermophilic archaebacteria, ES-4 (*25*), which grows up to 100°C, and *Thermococcus litoralis* (*22*), which grows up to 98°C, is also stimulated by tungsten. Moreover, cell extracts of these organisms contain high aldehyde oxidoreductase activity (S. Mukund and M. W. W. Adams, unpublished data, 1991). It will be of interest to characterize these enzymes and see how they compare with the AOR of *P. furiosus*.

As indicated in Fig. 18, all but one of the proteins involved in redox reactions in the proposed "pyroglycolytic" pathway of *P. furiosus* have been shown to contain Fe–S clusters. The properties of the hydrogenase, ferredoxin, and AOR have been described. In addition, POR has recently been purified from *P. furiosus* under strictly anaerobic conditions (J. Blamey and M. W. W. Adams, unpublished data, 1991). It is a trimeric protein ($\alpha\beta\gamma$, M_r 93,000) and contains approximately 8Fe atoms/mole. No other metals, including W, could be detected. EPR analysis of reduced POR indicates the presence of two $[4Fe–4S]^{1+}$ clusters, one of which has an $S = \frac{3}{2}$ ground state. The enzyme has half-life in air of about 15 min, and its optimum temperature for catalysis is above 90°C. POR has also been purified from several mesophilic organisms (*173–178*). In contrast to *P. furiosus* POR, these all have molecular weights of near 250,000 (usually as an α_2 dimer) and contain two or four $S = \frac{1}{2}$ $[4Fe–4S]^{1+}$ clusters. Whether the other oxidoreductase in the glycolytic pathway shown in Fig. 17, GOR, is also an Fe–S enzyme is not known at present.

IV. *Thermotoga maritima*

Thermotoga maritima is the most thermophilic eubacterium currently known. It was isolated by Stetter and co-workers from geothermally heated marine sediments in 1986 (*7*). The genus represents the oldest and most slowly evolving branch within the eubacterial kingdom (*8, 9*). The organism is a strict anaerobe and grows at temperatures up to 90°C by the fermentation of both simple and complex carbohydrates. It produces organic acids, CO_2, and H_2, and, like *P. furiosus,* appears to use the reduction of S^0 to H_2S as a means of removing H_2 rather than as a means of energy conservation. In our initial studies with this bacterium, we found that cell yields were increased twofold by the presence of additional Fe and of tungstate (10 μM) in the growth medium (*32*). The addition of salts of V, Cs, F, Pb, Rb, or Si, and increased amounts (>10 μM) of Ni, Mo, Se, Co, or Mn do not stimulate growth. In other words, W and Fe appear to have a similar effect on the growth of *T. maritima* as they do on *P. furiosus*. However, as will now be discussed, the role of these elements in the production of H_2 by *T. maritima* is quite different from what has been described in previous sections for *P. furiosus*.

A. Hydrogenase (Fe–S)

Thermotoga maritima contains a single hydrogenase located in the cytoplasm. It is routinely purified from cells grown in the presence of W (see Section IV,B) and absence of S^0 (*32*). The enzyme is very unstable in cell-free extracts at both 4 and 23°C, even under anaerobic and reducing conditions, and must be purified using buffers containing glycerol (10%, v/v) and dithiothreitol (2 mM) to prevent substantial losses in catalytic activity. The pure enzyme is a homotetramer (α_4) with a molecular weight of about 280,000. It is extremely sensitive to inactivation by O_2, having a half-life in air of 10 sec. It contains approximately 20 Fe and 18 S^{2-} atoms per monomer (M_r 68,000). Other metals, including Ni (and also Se), are present in only trace amounts. To date, hydrogenases lacking Ni have been purified and well characterized only from some mesophilic anaerobic bacteria. They are from the fermentative organisms, *C. pasteurianum,* in which two different Fe hydrogenases (termed I and II) are present (*179–183*), and *M. elsdenii* (*184–187*), and from the mesophilic sulfate reducer, *Desulfovibrio vulgaris* (*33, 188–192*). These are also soluble enzymes with molecular weights around 60,000, comparable to that of the monomer of the *T. maritima* enzyme, and in their active states they are also extremely

TABLE I

PROPERTIES OF Fe HYDROGENASES

	Source of hydrogenase[a]				
	Tm	Cp I	Cp II	Me	Dv
Molecular weight	280,000	62,000	54,000	58,000	55,820
Subunits:	4 × 68,000	—	—	—	1 × 45,820, 1 × 10,000
V_m, H_2 evolution[b]	164 (80°C)	5500	10	7000	10,400
V_m, H_2 oxidation[c]:	180 (80°C)	24,000	34,000	9,000	50,000
Fe/mole[d]	20	20	14	13–18	9–15
S^{2-}/mole[d]	18	18	11	16	13
Fe–S clusters[d]					
4Fe type					
($S = \frac{1}{2}$)	1	3	2	2	2
($S \geq \frac{3}{2}$)	1	1	—	—	—
2Fe type	2	—	—	—	—
Fe/mole available for the H cluster[d]	8	4	6	5–10	1–7
Ref.	*32*	*67, 179, 181, 183*	*180–183*	*184–184*	*188–192*

[a] Abbreviations: Tm, *T. maritima;* Cp I, hydrogenase I from *C. pasteurianum;* Cp II, hydrogenase II from *C. pasteurianum;* Me, *Megasphaera elsdenii;* Dv, *Desulfovibrio vulgaris* (strain Hildenborough).

[b] Expressed as micromoles of H_2 evolved/min/mg using dithionite-reduced methyl viologen as electron donor.

[c] Expressed as micromoles of H_2 oxidized/min/mg using methylene blue or benzyl viologen as the electron acceptor.

[d] Expressed per monomer for the *T. maritima* enzyme.

sensitive to inactivation by O_2. However, as might be expected, *T. maritima* Fe hydrogenase is much more thermostable. Its optimum temperature for H_2 production is above 95°C and it has a half-life at 90°C of about 1 hr. In contrast, the mesophilic enzymes denature in minutes at 70°C.

As shown in Table I, a major difference between the *T. maritima* and mesophilic Fe enzymes lies in their catalytic activities. The latter exhibit extremely high rates of H_2 oxidation and H_2 evolution in *in vitro* assays (the exception is H_2 evolution by *C. pasteurianum* hydrogenase II), and these are one to two orders of magnitude greater than those of the *T. maritima* enzyme, even at 80°C. In fact, the catalytic activities of *T. maritima* hydrogenase more resemble those of a Ni–Fe hydrogenase. In addition, the *T. maritima* enzyme shows "mixed" inhibition properties. It is as sensitive to inhibition by CO as the other Fe

hydrogenases ($K_i \leq 1\ \mu M$), but like Ni–Fe hydrogenases, *T. maritima* hydrogenase is insensitive to inhibition by nitrite (10 mM) but is inhibited by acetylene ($t_{1/2} \sim 20$ min under 1 atm C_2H_2). The mesophilic Fe enzymes are inhibited by nitrite ($K_i = 3\ \mu M$) but are unaffected by acetylene. A further difference between the *T. maritima* and mesophilic Fe hydrogenases lies in their physiological electron carriers. The hydrogenases of *C. pasteurianum* (I) and *M. elsdenii* evolve H_2 during cell growth and accept electrons from reduced ferredoxin *in vivo* (*179, 185*). In light of this, we recently purified a ferredoxin from *T. maritima* (J. Blamey and M. W. W. Adams, unpublished, 1991). Preliminary data indicate that it has a molecular weight of around 6000 and contains a single cluster. However, it did not serve as an electron donor to *T. maritima* hydrogenase in *in vitro* H_2 evolution assays, and the natural electron carrier for the enzyme is unknown.

As indicated in Table I, the Fe–S content of *T. maritima* hydrogenase (per monomer) is comparable to what has been reported for the other Fe hydrogenases. However, in contrast to the mesophilic enzymes, *T. maritima* hydrogenase in its reduced state exhibits EPR signals at high temperatures (60 K; see Fig. 19). A power saturation study showed that these resonances arise from two different species (*32*), and from their spin content, g values, and relaxation properties, they are assigned to two different $S = \frac{1}{2}$ $[2Fe–2S]^{1+}$ clusters. Additional resonances are observed when the temperature is reduced to 10 K (Fig. 19) and these arise from at least one $S = \frac{1}{2}$ $[4Fe–4S]^{1+}$ cluster. EPR is also observed from reduced *T. maritima* hydrogenase at low field and low temperature (Fig. 19). The major feature at $g = 5.7$ most likely originates from an $S = \frac{3}{2}$ $[4Fe–4S]^{1+}$ cluster, but the g values and temperature dependence of other resonances are inconsistent with an isolated $S = \frac{3}{2}$ system (for discussion, see Ref. *32*). The EPR data therefore indicate that *T. maritima* hydrogenase contains two 4Fe centers, one $S = \frac{1}{2}$ and one in two or more spin states ($S \geq \frac{3}{2}$), in addition to two 2Fe centers. The E_m values (pH 8.0, 20°C) of the 2Fe- and 4Fe-type clusters are -440 and -390 mV, respectively. Ferredoxin-type 2Fe clusters are not present in the mesophilic Fe hydrogenases: they all contain $S = \frac{1}{2}$ [4Fe–4S] clusters (*C. pasteurianum* hydrogenase I also has one $S = \frac{3}{2}$ 4Fe cluster; Ref. *67*).

As mentioned in Section III,A, the site of H_2 oxidation and H_2 evolution in the mesophilic Fe hydrogenases is thought to be a novel Fe–S cluster, termed the H cluster (for review, see Ref. *38*). Of unknown structure, it contains at least three and possibly six Fe atoms (*38, 183*). It has an E_m value of -400 mV (pH 8.0), is diamagnetic ($S = 0$) in the reduced state, and in the oxidized state ($S = \frac{1}{2}$) exhibits a characteristic

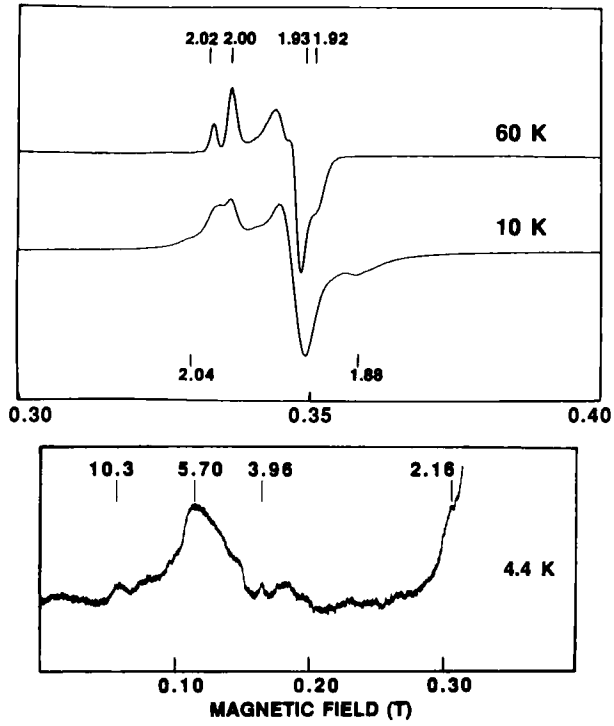

FIG. 19. EPR spectra of the Fe hydrogenase of *T. maritima*. The hydrogenase (10 mg/ml) was reduced with sodium dithionite (2 m*M*). Spectra were recorded at 4.4, 10, and 60 K as indicated using microwave power of 10 mW (upper panel) and 50 mW (lower panel: relative gain, times 40). Modified from Ref. *32*.

rhombic EPR signal with $g_{av} > 2$. However, *T. maritima* hydrogenase in its oxidized state is EPR silent, and no EPR signals in addition to those of the ferredoxin-type centers are apparent during a redox titration (*32*). This was very surprising considering that the 4Fe and 2Fe centers in this enzyme account for only 12 iron atoms/monomer. This leaves up to 8 iron atoms/mole for an H cluster, but the remaining iron in *T. maritima* hydrogenase is not detectable by EPR spectroscopy. When one also considers the differences between the *T. maritima* enzyme and the mesophilic Fe hydrogenases in their catalytic activities and sensitivity to inhibitors (Table I), these data suggest that *T. maritima* hydrogenase has a catalytic Fe–S cluster that is different from the H cluster of the mesophilic enzymes. Why this site is EPR silent, however, remains to be established. It is relevant to mention that a

puzzling property of the mesophilic Fe enzymes is that, when oxidized, they give rise to paramagnetic MCD bands that arise from a center with an $S > \frac{1}{2}$ ground state, even though the only paramagnet detectable by EPR and Mössbauer spectroscopy is the $S = \frac{1}{2}$ oxidized H cluster (*38, 67*). Preliminary MCD studies of the oxidized *T. maritima* enzyme show that is also exhibits paramagnetic MCD (R. C. Conover, A. Juszczak, M. W. W. Adams, and M. K. Johnson, unpublished data, 1991). This suggests a possible relationship between its H_2-activating center and the H cluster of the mesophilic enzymes. In addition, as already discussed (Section III,B,3), the H cluster of *C. pasteurianum* hydrogenase I has substantial noncysteinyl (nitrogenous) coordination (*97*). The finding of much less cysteine (12 per monomer) than iron in *T. maritima* hydrogenase suggests that this may also be the case for the H cluster of this enzyme.

B. Role of Tungsten

The presence of W in the growth medium of *T. maritima* was found to increase both the cellular concentration of the hydrogenase in cell-free extracts, and also its catalytic activity *in vitro* (*32*). For example, cells from W-supplemented media yield approximately 200 mg of pure hydrogenase/kg (wet weight), and the enzyme has a specific activity in the standard H_2 evolution assay of $\geq$50 units/mg. If W is omitted, the yield drops to around 100 mg/kg, and the specific activity of the final preparation is at least an order of magnitude lower, usually around 4 units/mg. However, there are no detectable differences in the physical properties of the two types of hydrogenases (from cells with and without W). That is, the EPR properties (both oxidized and reduced) and the Fe and S^{2-} content of the hydrogenase from cells grown without added W are the same as those of the enzyme described in Section III,A. It is possible that the H_2-activating Fe–S center is quite different in these two forms of *T. maritima* hydrogenase, but since this cluster is not detectable by EPR spectroscopy, other techniques such as Mössbauer spectroscopy will be needed to determine if this is the case.

These results suggest that W directly influences both the amount of hydrogenase in *T. maritima* cells and the integrity of its catalytic Fe–S cluster, and lead to the obvious question: why, and what is the role of W in this organism? Like *P. furiosus*, *T. maritima* grows by fermenting carbohydrates and evolving H_2, and the likely answer is that it contains a W-dependent glycolytic pathway analogous to that shown in Fig. 18. However, this is not the case, as *T. maritima* does not contain detectable aldehyde (or glucose) oxidoreductase activity (*32*). W could well be a

component of a key enzyme in yet another version of an H_2-evolving glycolytic pathway, and its effect on *T. maritima* hydrogenase would be consistent with this. At present though, the function of W in the metabolism of *T. maritima* is a mystery.

Finally we turn to the question of why extremely thermophilic archaebacteria, such as *P. furiosus, T. litoralis,* and "ES-4," and the most thermophilic eubacterium currently known, *T. maritima,* depend upon W for optimal growth, when the rest of the microbial world, indeed, the rest of biology, uses Mo as a key comonent of the active sites of a wide variety of important enzymes (e.g., Refs. *166, 167,* and *193*). In fact, since extreme thermophily is regarded as an ancient phenotype (*8, 9*), one could speculate that the earliest life forms were not only extremely thermophilic, they were also W-dependent organisms. Presumably, they then evolved into the mesophilic, Mo-dependent species that now overwhelmingly predominate. As to the W requirement, it is possible that W but not Mo is present in the environments in which extreme thermophilic organisms are found, such as near deep-sea hydrothermal vents. Alternatively, W may be easier to stabilize at extreme temperatures in the oxidation states and at the redox potentials required to catalyze biologically relevant reactions. However, as yet there is no experimental evidence to support either of these possibilities.

V. Summary

In this article the properties of some of the Fe–S enzymes and proteins involved in the production of H_2 by some extremely thermophilic bacteria have been described. The hyperthermophilic archaebacterium, *P. furiosus,* which grows optimally at 100°C, contains an extremely thermostable Ni–Fe hydrogenase that is uniquely primed to catalyze the physiological reaction, H_2 production. Its active site Ni appears to be redox active only at high temperatures, whereas the redox properties of its 2Fe and 4Fe clusters seem insensitive to temperature. The physiological electron donor for this hydrogenase is an extremely thermostable 4Fe ferredoxin. The lack of complete cysteinyl coordination to its cluster enables other ligands to bind to the unique Fe site, the facile removal of this Fe atom, and its replacement with other metal ions, in particular Ni. Such [M–3Fe–4S] clusters in an extremely stable protein may prove to be useful models for the catalytic sites of several Fe–S enzymes. Tungsten, an element seldom used in biology, stimulates the growth of *P. furiosus,* and from it a novel tungstopterin-containing Fe–S enzyme has been characterized. The enzyme exhibits unique EPR

properties that arise from the spin coupling of two nonidentical Fe–S centers, and it is proposed to function as a glyceraldehyde ferredoxin oxidoreductase in a new glycolytic pathway. A unique aspect of this pathway, which appears also to be present in other extremely thermophilic archaebacteria, is that glucose can be oxidized to acetate without the participation of thermolabile nicotinamide nucleotides. An extremely thermostable rubredoxin has also been purified from *P. furiosus*. Preliminary NMR studies of the Zn-substituted protein is currently providing the first insights into the mechanisms of protein "hyperthermostability." The production of H_2 by the most thermophilic eubacterium currently known, *T. maritima,* is catalyzed by a new type of "Fe-only" hydrogenase. This differs from mesophilic Fe hydrogenases in its low catalytic activity, its sensitivity to inhibitors, its physiological electron carrier, and in the presence of 2Fe centers. It appears to contain a new type of Fe–S center for catalyzing H_2 production. The activity and cellular concentration of the hydrogenase in *T. maritima* is increased by the presence of W in the growth medium, However, this organism lacks the W-dependent "pyroglycolytic" pathway found in *P. furiosus,* and the role of W in its metabolism is unknown.

ACKNOWLEDGMENTS

I am indebted to the following persons for their contributions to much of the work described here and for many helpful discussions: Drs. M. K. Johnson, M. F. Summers, G. N. George, R. C. Prince, E. P. Day, J. B. Howard, B. M. Hoffman, and E. Münck. Research carried out in the author's laboratory was supported by grants from the Department of Energy, the Office of Naval Research, and the National Science Foundation.

REFERENCES

1. Stetter, K. O., *in* "The Thermophiles" (T. D. Brock, ed.), p. 39. Wiley, New York, 1986.
2. Kelly, R. M., and Deming, J. W., *Biotech. Prog.* **4,** 47 (1988).
3. Stetter, K. O., Fiala, G., Huber, G., Huber, R., and Segerer, G., *FEMS Microbiol. Rev.* **75,** 117 (1990).
4. Adams, M. W. W., *FEMS Microbiol. Rev.* **75,** 219 (1990).
5. Wiegel, J. K. W., and Ljungdahl, L. G., *Crit. Rev. Biotechnol.* **3,** 39 (1986).
6. Stetter, K. O., *Nature (London)* **300,** 258 (1982).
7. Huber, R., Langworthy, T. A., König, H., Thomm, M., Woese, C. R., Sleytr, U. B., and Stetter, K. O., *Arch. Microbiol.* **144,** 324 (1986).
8. Woese, C. R., Kandler, O., and Wheelis, M. L., *Proc. Natl. Acad. Sci. U.S.A.* **87,** 4576 (1990).

9. Woese, C. R., *Microbiol. Rev.* **51,** 221 (1987).
10. Stetter, K. O., and Zillig, W., *in* "The Bacteria" (C. R. Woese and R. S. Wolfe, eds.), Vol. 8, p. 85. Academic Press, New York, 1985.
11. Fiala, G., Stetter, K. O., Jannasch, H. W., Langworthy, T. A., and Madon, J., *Syst. Appl. Microbiol.* **8,** 106 (1986).
12. Jannasch, H. W., Wirsen, C. O., Molyneaux, S. J., and Langworthy, T. A., *Appl. Environ. Microbiol.* **54,** 1203 (1988).
13. Zillig, W., Gierl, S., Schreiber, G., Wunderl, S., Janekovic, D., Stetter, K. O., and Klenk, H. P., *Syst. Appl. Microbiol.* **4,** 79 (1983).
14. Huber, R., Kristjansson, J. K., and Stetter, K. O., *Arch. Microbiol.* **149,** 95 (1987).
15. Segerer, A., Neuner, A., Kristjansson, J. K., and Stetter, K. O., *Int. J. Syst. Bacteriol.* **36,** 559 (1986).
16. Zillig, W., Yeats, S., Holz, I., Böck, A., Rettenberger, M., Gropp, F., and Simon, G., *Syst. Appl. Microbiol.* **8,** 197 (1986).
17. Stetter, K. O., König, H., and Stackebrandt, E., *Syst. Appl. Microbiol.* **4,** 535 (1983).
18. Pley, U., Schipka, J., Gambacorta, A., Jannasch, H. W., Fricke, H., Rachel, R., and Stetter, K. O., *Syst. Appl. Microbiol.* **14,** 245 (1991).
19. Fiala, G., and Stetter, K. O., *Arch. Microbiol.* **145,** 56 (1986).
20. Zillig, W., Holz, I., Klenk, H.-P., Trent, J., Wunderl, D., Janekovic, D., Imsel, E., and Hass, B., *Syst. Appl. Microbiol.* **9,** 62 (1987).
21. Zillig, W., Holtz, I., Janekovic, D., Schafer, W., and Reiter, W. D., *Syst. Appl. Microbiol.* **4,** 88 (1983).
22. Neuner, A., Jannasch, H., Belkin, S., and Stetter, K. O., *Arch. Microbiol.* **153,** 205 (1990).
23. Zillig, W., Holz, I., and Wunderl, S., *Int. J. Syst. Bacteriol.* **41,** 169 (1991).
24. Pledger, R. J., and Baross, J. A., *Syst. Appl. Microbiol.* **12,** 249 (1989).
25. Pledger, R. J., and Baross, J. A., *J. Gen. Microbiol.* **137,** 203 (1990).
26. Huber, R., Kurr, M., Jannasch, H. W., and Stetter, K. O., *Nature (London)* **342,** 833 (1989).
27. Jones, W. J., Leigh, J. A., Moyer, F., Woese, C. R., and Wolfe, R. S., *Arch. Microbiol.* **136,** 254 (1983).
28. Stetter, K. O., Thomm, M., Winter, J., Wildegruber, G., Huber, H., Zillig, W., Janekovic, D., König, H., Palm, P., and Wunderl, S., *Zbl. Bakt. Hyg., I Abt. Orig.* **C2,** 166 (1981).
29. Lauerer, G., Kristjansson, J. K., Langworthy, T. A., König, H., and Stetter, K. O., *Syst. Appl. Microbiol.* **8,** 100 (1986).
30. Stetter, K. O., Lauerer, G., Thomm, M., and Neuner, A., *Science* **236,** 822 (1987).
31. Bryant, F. O., and Adams, M. W. W., *J. Biol. Chem.* **264,** 5070 (1989).
32. Juszczak, A., Aono, S., and Adams, M. W. W., *J. Biol. Chem.* **266,** 13834 (1991).
33. Fauque, G., Peck, H. D., Jr., Moura, J. J. G., Huynh, B. H., Berlier, Y., DerVartanian, D. V., Teixeira, M., Przybyla, A., Lespinat, P. A., Moura, I., and LeGall, J., *FEMS Microbiol. Rev.* **54,** 299 (1989).
34. Tran-Betcke, A., Warnecke, U., Böcker, C., Zaborosch, C., and Friedrich, B., *J. Bacteriol.* **172,** 2920 (1990).
35. Kovacs, K. L., Seefeldt, L. C., Tigyi, G., Doyle, C. M., Mortenson, L. E., and Arp, D. J., *J. Bacteriol.* **171,** 430 (1989).
36. Kojima, N., Fox, J. A., Hausinger, R. P., Daniels, L., Orme-Johnson, W. H., and Walsh, C., *Proc. Natl. Acad. Sci. U.S.A.* **80,** 378 (1983).
37. Schneider, K., Cammack, R., and Schlegel, H. G., *Eur. J. Biochem.* **142,** 75 (1984).
38. Adams, M. W. W., *Biochim. Biophys. Acta* **1020,** 115 (1990).

39. Cammack, R., Fernandez, V. M., and Schneider, K., *in* "Bioinorganic Chemistry of Nickel" (J. R. Lancaster, Jr., ed.), p. 167. VCH Publ., Deerfield Beach, Florida, 1988.
40. Hausinger, R. P., *Microbiol. Rev.* **51,** 22 (1987).
41. Cammack, R., Bagyinka, C., and Kovacs, K. L., *Eur. J. Biochem.* **182,** 357 (1989).
42. Van der Zwaan, J. W., Albracht, S. P. J., Fontijn, R. D., and Mul, P., *Eur. J. Biochem.* **169,** 377 (1987).
43. Schneider, K., Cammack, R., and Schlegel, H. G., *Eur. J. Biochem.* **142,** 75 (1984).
44. Teixeira, M., Moura, I., Xavier, A. V., Moura, J. J. G., LeGall, J., DerVartanian, D. V., Peck, H. D., Jr., and Huynh, B. H., *J. Biol. Chem.* **264,** 16435 (1989).
45. Cammack, R., Patil, D. S., and Fernandez, V. M., *Biochem. Soc. Trans.* **13,** 572 (1985).
46. Coremans, J. M. C. C., Van der Zwaan, J. W., and Albracht, S. P. J., *Biochim. Biophys. Acta* **997,** 256 (1989).
47. Park, J.-B., Fan, C., Hoffman, B. M., and Adams, M. W. W., *J. Biol. Chem.* **266,** 19351 (1991).
48. Hyman, M. R., and Arp, D. J., *Anal. Biochem.* **173,** 207 (1988).
49. Aono, S., Bryant, F. O., and Adams, M. W. W., *J. Bacteriol.* **171,** 3433 (1989).
50. Sato, S., Nakazawa, K., Hon-nami, K., and Oshima, T., *Biochim. Biophys. Acta* **668,** 277 (1981).
51. Terlesky, K. C., and Ferry, J. G., *J. Biol. Chem.* **263,** 4080 (1988).
52. Yang, S.-S., Ljungdahl, L. G., and LeGall, J., *J. Bacteriol.* **130,** 1084 (1977).
53. Brushi, M., and Guerlesquin, F., *FEMS Microbiol. Rev.* **54,** 155 (1988).
54. Saeki, K., Yao, Y., Wakabayashi, S., Shen, G.-J., Zeikus, J. G., and Matsubara, H., *J. Biochem. (Tokyo)* **106,** 656 (1989).
55. Schatt, E., Jouanneau, Y., and Vignais, P. M., *J. Bacteriol.* **171,** 6218 (1989).
56. Okawara, N., Ogata, M., Yagi, T., Wakabayashi, S., and Matsubara, H., *J. Biochem. (Tokyo)* **104,** 196 (1988).
57. Bovier-Lapierre, G., Bruschi, M., Bonicel, J., and Hatchikian, E. C., *Biochim. Biophys. Acta* **913,** 20 (1987).
58. Wakabayashi, S., Fujimoto, N., Wada, K., Matsubara, H., Kerscher, L., and Oesterhelt, D., *FEBS Lett.* **162,** 21 (1983).
59. Minami, Y., Wakabayashi, S., Wada, K., Matsubara, H., Kersher, L., and Oesterhelt, D., *J. Biochem. (Tokyo)* **97,** 745 (1983).
60. Orme-Johnson, W. H., and Sands, R. H., *in* "Iron-Sulfur Proteins" (W. Lovenberg, ed.), Vol. 2, p. 185. Academic Press, New York, 1977.
61. Matthews, R., Charlton, S., Ssnds, R. H., and Palmer, G., *J. Biol. Chem.* **249,** 4326 (1974).
62. Conover, R. C., Kowal, A. T., Fu, W., Park, J.-B., Aono, S., Adams, M. W. W., and Johnson, M. K., *J. Biol. Chem.* **265,** 8533 (1990).
63. Armstrong, F. A., George, S. J., Cammack, R., Hatchikian, E. C., and Thomson, A. J., *Biochem. J.* **264,** 265 (1989).
64. Lindahl, P. A., Day, E. P., Kent, T. A., Orme-Johnson, W. H., and Münck, E., *J. Biol. Chem.* **260,** 11160 (1985).
65. Hagen, W. R., Eady, R. R., Dunham, W. R., and Haaker, H., *FEBS Lett.* **189,** 250 (1985).
66. Watt, G. D., and McDonald, J. W., *Biochemistry* **24,** 7226 (1985).
67. Zambrano, I. C., Kowal, A. T., Mortenson, L. E., Adams, M. W. W., and Johnson, M. K., *J. Biol. Chem.* **264,** 20974 (1989).
68. Onate, Y. A., Vollmer, S. J., Switzer, R. L., and Johnson, M. K., *J. Biol. Chem.* **264,** 18386 (1989).

69. Makaroff, C. A., Zalkin, H., Switzer, R. L., and Vollmer, S. J., *J. Biol. Chem.* **258,** 10586 (1983).
70. Hausinger, R., and Howard, J. B., *J. Biol. Chem.* **258,** 13486 (1983).
71. Howard, J. B., Davis, R., Moldenhauer, B., Cash, V. L., and Dean, D., *J. Biol. Chem.* **264,** 11270 (1989).
72. Kennedy, M. C., Werst, M., Telser, J., Emptage, M. H., Beinert, H., and Hoffman, B. M., *Proc. Natl. Acad. Sci. U.S.A.* **84,** 8854 (1987).
73. Emptage, M. H., Dreyer, J.-L., Kennedy, M. C., and Beinert, H., *J. Biol. Chem.* **258,** 11106 (1983).
74. Armstrong, F. A., Hill, H. A. O., and Walton, N. J., *Q. Rev. Biophys.* **18,** 261 (1986).
75. Robbins, A. H., and Stout, C. D., *Proteins: Struct. Funct. Genet.* **5,** 289 (1989).
76. Beinert, H., and Kennedy, M. C., *Eur. J. Biochem.* **186,** 5 (1989).
77. Werst, M. M., Kennedy, M. C., Beinert, H., and Hoffman, B. M., *Biochemistry* **29,** 1026 (1990).
78. Carney, M. J., Papaefthymiou, G. C., Spartalian, K., Frankel, R. B., and Holm, R. H., *J. Am. Chem. Soc.* **110,** 6084 (1988).
79. Johnson, M. K., Robinson, A. E., and Thomson, A. J., *in* "Iron-Sulfur Proteins" (T. G. Spiro, ed.), Vol. 4, p. 367. Wiley, New York, 1982.
80. Finnegan, M. G., Onate, Y. A., Hales, B. J., Switzer, R. L., and Johnson, M. K., *J. Inorg. Biochem.* **36,** 251 (1989).
81. Czernuszewicz, R. S., Macor, K. A., Johnson, M. K., Gewirth, A., and Spiro, T. G., *J. Am. Chem. Soc.* **109,** 7178 (1987).
82. Spiro, T. G., Czernuszewicz, R. S., and Han, S., *in* "Biological Applications of Raman Spectroscopy" (T. G. Spiro, ed.), Vol. 3, p. 523. Wiley, New York, 1988.
83. Madden, J. F., Han, S., Siegel, L. M., and Spiro, T. G., *Biochemistry* **28,** 5471 (1989).
84. Kissinger, C. R., Adman, E. T., Sieker, L. C., Jensen, L. H., and LeGall, J., *FEBS Lett.* **244,** 447 (1989).
85. Kissinger, C. R., Sieker, L. C., Adman, E. T., and Jensen, L. H., *J. Mol. Biol.* **219,** 693 (1991).
86. Kent, T. A., Dreyer, J.-L., Kennedy, M. C., Huynh, B. H., Emptage, M. H., Beinert, H., and Münck, E., *Proc. Natl. Acad. Sci. U.S.A.* **79,** 1096 (1982).
87. Thomson, A. J., Robinson, A., Johnson, M. K., Cammack, R., Rao, K. K., and Hall, D. O., *Biochim. Biophys. Acta* **637,** 423 (1981).
88. Moura, J. J. G., Moura, I., Kent, T. A., Lipscomb, J. D., Huynh, B. H., LeGall, J., Xavier, A. V., and Münck, E., *J. Biol. Chem.* **257,** 6259 (1982).
89. Cunningham, R. P., Asahara, H., Bank, J. F., Scholes, C. P., Salerno, J. C., Surerus, K., Münck, E., McCracken, J., Pesiach, J., and Emptage, M. H., *Biochemistry* **28,** 4450 (1989).
90. Vollmer, S. J., Switzer, R. L., and Debrunner, P. G., *J. Biol. Chem.* **258,** 14284 (1983).
91. Holm, R. H., and Simhon, E. D., *in* "Molybdenum Enzymes" (T. G. Spiro, ed.), p. 1. Wiley, New York, 1985.
91a. Adams, M. W. W., Rao, K. K., Hall, D. O., Christou, G., and Garner, G., *Biochim. Biophys. Acta* **589,** 1 (1980).
92. Flint, D. H., and Emptage, M. H., *J. Biol. Chem.* **263,** 3558 (1988).
93. Scopes, R. K., and Griffiths-Smith, K., *Anal. Biochem.* **136,** 530 (1984).
94. Dreyer, J.-L., *Eur. J. Biochem.* **150,** 145 (1985).
95. Kuchta, R. D., Hanson, G. R., Holmquist, B., and Abeles, R. H., *Biochemsitry* **25,** 7301 (1986).
96. Kelly, J. M., and Scopes, R. K., *FEBS Lett.* **202,** 274 (1986).

97. Thomann, H., Bernadino, M., and Adams, M. W. W., *J. Am. Chem. Soc.* **113,** 7044 (1991).
98. Nelson, M. J., Levy, M. A., and Orme-Johnson, W. H., *Proc. Natl. Acad. Sci. U.S.A.* **80,** 147 (1983).
99. Orme-Johnson, W. H., *Annu. Rev. Biophys. Chem.* **14,** 419 (1985).
100. Holm, R. H., and Simhon, E. D., *in* "Molybdenum Enzymes" (T. G. Spiro, ed.), p. 1. Wiley, New York, 1985.
101. Challen, P. R., Koo, S.-M., Kim, C. G., Dunham, W. R., and Coucouvanis, D., *J. Am. Chem. Soc.* **112,** 8606 (1990).
102. Smith, B. E., Eady, R. R., Lowe, D. J., and Gormal, C., *Biochem. J.* **250,** 299 (1988).
103. Ciurli, S., and Holm, R. S., *Inorg. Chem.* **28,** 1685 (1989).
104. Chisnell, J. R., Premakumar, R., and Bishop, P. E., *J. Bacteriol.* **170,** 27 (1988).
105. Thomann, H., Morgan, T. V., Jin, H., Burgmayer, S. J. N., Bare, R. E., and Stiefel, E. I., *J. Am. Chem. Soc.* **109,** 7913 (1987).
106. Ragsdale, S. W., Wood, H. G., and Antholine, W. E., *Proc. Natl. Acad. Sci. U.S.A.* **82,** 6811 (1985).
107. Terlesky, K. C., Barber, M. J., Aceti, D. J., and Ferry, J. G., *J. Biol. Chem.* **262,** 15392 (1987).
108. Cramer, S. P., Eidsness, M. K., Pan, W.-H., Morton, T. A., Ragsdale, S. W., DerVartanian, D. V., Ljungdahl, L. G., and Scott, R. A., *Inorg. Chem.* **26,** 2477 (1987).
109. Bastian, N. R., Diekert, G., Niederhoffer, E. C., Teo, B.-K., Walsh, C. T., and Orme-Johnson, W. H., *J. Am. Chem. Soc.* **110,** 5581 (1988).
110. Stephens, P. J., McKenna, M.-C., Ensign, S. A., Bonam, D., and Ludden, P. A., *J. Biol. Chem.* **264,** 16347 (1989).
111. Ensign, S. A., Campbell, M. J., and Ludden, P. W., *Biochemistry* **29,** 2162 (1990).
112. Fan, C., Gorst, C. M., Ragsdale, S. W., and Hoffman, B. M., *Biochemistry* **30,** 431 (1991).
113. Lindahl, P. A., Ragsdale, S. W., and Münck, E., *J. Biol. Chem.* **265,** 3880 (1990).
114. R. H. Holm, This volume.
115. Challen, P. R., Koo, S.-M., Kim, C. G., Dunham, W. R., and Coucouvanis, D., *J. Am. Chem. Soc.* **112,** 8606 (1990).
116. Stack, T. D. P., and Holm, R. H., *J. Am. Chem. Soc.* **110,** 2484 (1988).
117. Stack, T. D. P., Carney, M. J., and Holm, R. H., *Inorg. Chem.* **111,** 1670 (1989).
118. Weigel, J. A., Strivastave, K. K. P., Day, E. P., Münck, E., and Holm, R. H., *J. Am. Chem. Soc.* **112,** 8015 (1990).
119. Berg, J. M., and Holm, R. H., *in* "Iron Sulfur Proteins" (T. G. Spiro, ed.), p. 1. Wiley, New York, 1982.
120. Moura, I., Moura, J. J. G., Münck, E., Papaefthymiou, V., and LeGall, J., *J. Am. Chem. Soc.* **108,** 349 (1986).
121. Surerus, K. K., Münck, E., Moura, I., Moura, J. J. G., and LeGall, J., *J. Am. Chem. Soc.* **109,** 2805 (1987).
122. Conover, R. C., Park, J.-B., Adams, M. W. W., and Johnson, M. K., *J. Am. Chem. Soc.* **112,** 4562 (1990).
123. Surerus, K. K., Ph.D. Dissertation, University of Minnesota, Minneapolis, Minnesota (1989).
124. Ciurli, S., Yu, S., Holm, R. H., Srivastava, K. K. P., and Münck, E., *J. Am. Chem. Soc.* **112,** 8169 (1990).
125. Ensign, S. A., Hyman, M. R., and Ludden, P. W., *Biochemistry* **28,** 4973 (1989).
126. Carney, M. J., Kovacs, J. A., Zhang, Y.-P., Papaefthymiou, G. C., Spartalian, K., Frankel, R. B., and Holm, R. H., *Inorg. Chem.* **26,** 719 (1987).

127. Conover, R. C., Park, J.-B., Adams, M. W. W., and Johnson, M. K., *J. Am. Chem. Soc.* **113,** 2799 (1991).
128. Yasunobu, K. T., and Tanaka, M., *in* "Iron-Sulfur Proteins" (W. Lovenberg, ed.), Vol. 2, p. 27. Academic Press, New York, 1973.
129. Watenpaugh, K. D., Sieker, L. C., Herriott, J. R., and Jensen, L. H., *Acta Crystallogr.* **B29,** 943 (1973).
130. Seki, Y., Seki, S., Satoh, M., Ikeda, A., and Ishimoto, M., *J. Biochem. (Tokyo)* **106,** 336 (1989).
131. Meyer, J., Gagnon, J., Sieker, L. C., van Dorsselaer, A., and Moulis, J.-M., *Biochem. J.* **271,** 839 (1990).
132. Woolley, K. J., and Meyer, T. E., *Eur. J. Biochem.* **163,** 161 (1987).
133. Bruschi, M., *Biochim. Biophys. Acta* **434,** 4 (1976).
134. Voordouw, G., *Gene* **69,** 75 (1988).
135. Shimizu, F., Ogata, M., Yagi, T., Wakabayashi, S., and Matsubara, H., *Biochimie* **71,** 1171 (1989).
136. Bruschi, M., *Biochem. Biophys. Res. Commun.* **70,** 615 (1976).
137. Hormel, S., Walsh, K. A., Prickril, B. C., Titani, K., LeGall, J., and Sieker, L. C., *FEBS Lett.* **201,** 147 (1986).
138. Bachmeyer, H., Yasunobu, K. T., Peel, J. L., and Mayhew, S., *J. Biol. Chem.* **243,** 1022 (1968).
139. Bachmeyer, H., Benson, A. M., Yasunobu, K. T., Garrard, W. T., and Whiteley, H. R., *Biochemistry* **7,** 986 (1968).
140. Saeki, K., Yao, Y., Wakabayashi, S., Shen, G.-J., Zeikus, J. G., and Matsubara, H., *J. Biochem. (Tokyo)* **106,** 336 (1989).
141. Adman, E. T., Sieker, L. C., Jensen, L. H., Bruschi, M., and LeGall, J., *J. Mol. Biol.* **112,** 113 (1977).
142. Watenpaugh, K. D., Sieker, L. C., and Jensen, L. H., *J. Mol. Biol.* **131,** 509 (1979).
143. Sieker, L. C., Stenkamp, R. E., Jensen, L. H., Prickril, B., and LeGall, J., *FEBS Lett.* **208,** 73 (198).
144. Blake, P. R., Park, J.-B., Bryant, F. O., Aono, S., Magnuson, J. K., Eccleston, E., Howard, J. B., Summers, M. F., and Adams, M. W. W., *Biochemistry,* **30,** 10885 (1991).
145. Dutton, P. L., *in* "Methods in Enzymology" (S. Fleischer and L. Packer, eds.), Vol. 54, p. 411. Academic Press, New York, 1978.
146. Koller, K. B., and Hawkridge, F. M., *J. Electroanal. Chem.* **239,** 291 (1988).
147. Lovenberg, W., and Sobel, B. E., *Proc. Natl. Acad. Sci. U.S.A.* **54,** 193 (1965).
148. Papavassiliou, P., and Hatchikian, E. C., *Biochim. Biophys. Acta* **810,** 1 (1985).
149. Zwickl, P., Fabry, S., Bogedain, C., Haas, A., and Hensel, R., *J. Bacteriol.* **172,** 4329 (1990).
150. Summers, M. F., South, T. L., Kim, B., and Hare, D. R., *Biochemistry* **29,** 329 (1990).
151. Ragsdale, S. W., Ljungdahl, L. G., and DerVartanian, D. V., *J. Bacteriol.* **155,** 1224 (1983).
152. Hugenholtz, J., and Ljungdahl, L. G., *FEMS Microbiol. Rev.* **87,** 383 (1990).
153. Saeki, K., Jain, M. K., Shen, G.-J., Prince, R. C., and Zeikus, J. G., *J. Bacteriol.* **171,** 4736 (1989).
154. Stewart, D. E., LeGall, J., Moura, I., Moura, J. J. G., Peck, H. D., Jr., Xavier, A. V., Weiner, P. K., and Wampler, J. E., *Eur. J. Biochem.* **185,** 695 (1989).
155. Thomson, A. J., *FEBS Lett.* **286,** 230 (1991).
156. Mukund, S., and Adams, M. W. W., *J. Biol. Chem.* **265,** 11508 (1990).
157. Yamamoto, I., Saiki, T., Liu, S.-M., and Ljungdahl, L. G., *J. Biol. Chem.* **258,** 1826 (1983).

158. Clark, W. M., "Oxidation Reduction Potentials of Organic Systems." Kruger Publ., Huntingdon, New York, 1972.
159. Wood, P. M., *Trends Biochem. Sci.* **10,** 106 (1985).
160. Prince, R. C., and Adams, M. W. W., *J. Biol. Chem.* **262,** 5125 (1987).
161. Mayhew, S. G., *Eur. J. Biochem.* **85,** 535 (1978).
162. Thauer, R. K., Jungermann, K., and Decker, K., *Bacteriol. Rev.* **41,** 100 (1977).
163. Loach, P. A., *in* "Handbook of Biochemistry and Molecular Biology" (G. D. Fasman, ed.), Vol. 1, p. 122. CRC Press, Cleveland, Ohio, 1976.
164. Mukund, S., and Adams, M. W. W., *J. Biol. Chem.* **266,** 14208 (1991).
165. George, G. N., Prince, R. P., Mukund, S., and Adams, M. W. W., *J. Am. Chem. Soc.* in press (1991).
166. Coughlan, M. P., *in* "Molybdenum and Molybdenum-Containing Enzymes" (M. P. Coughlan, ed.), p. 119. Pergamon, New York, 1980.
167. Hille, R., and Massey, V., *in* "Molybdenum Enzymes" (T. G. Spiro, ed.), p. 443. Wiley, New York, 1985.
168. George, G. N., Kipke, C. A., Prince, R. C., Sunde, R. A., Enemark, J. H., and Cramer, S. P., *Biochemistry* **28,** 5075 (1989).
169. De Rosa, M., Gambacorta, R., Nicolaus, B., Giardina, P., Poerio, E., and Buonocore, V., *Biochem. J.* **224,** 407 (1984).
170. Budgen, N., and Danson, M. J., *FEBS Lett.* **196,** 207 (1986).
171. Danson, M. J., *Adv. Microbiol. Physiol.* **29,** 165 (1989).
172. Dawson, R. M. C., Elliott, D. C., Elliott, W. H., and Jones, K. M., eds., *in* "Data for Biochemical Research," 3rd Ed. Oxford Univ. Press (Clarendon) Oxford, 1986.
173. Uyeda, K., and Rabinowitz, J. C., *J. Biol. Chem.* **246,** 3111 (1971).
174. Kerscher, L., and Oesterhelt, D., *Eur. J. Biochem.* **116,** 587 (1981).
175. Drake, H. L., Hu, S.-I., and Wood, H. G., *J. Biol. Chem.* **256,** 11137 (1981).
176. Wahl, R. C., and Orme-Johnson, W. H., *J. Biol. Chem.* **262,** 10489 (1987).
177. Williams, K., Lowe, P. N., and Leadlay, P. F., *Biochem. J.* **246,** 529 (1987).
178. Meinecke, B., Bertram, J., and Gottschalk, G., *Arch. Microbiol.* **152,** 244 (1989).
179. Chen, J.-S., and Mortenson, L. E., *Biochim. Biophys. Acta* **371,** 283 (1974).
180. Chen, J.-S., and Blanchard, D. K., *Biochem. Biophys. Res. Commun.* **84,** 1144 (1978).
181. Adams, M. W. W., and Mortenson, L. E., *J. Biol. Chem.* **259,** 7045 (1984).
182. Adams, M. W. W., and Mortenson, L. E., *Biochim. Biophys. Acta* **766,** 51 (1984).
183. Adams, M. W. W., Eccleston, E., and Howard, J. B., *Proc. Natl. Acad. Sci. U.S.A.* **86,** 4932 (1989).
184. Grande, H. J., Dunham, W. R., Averill, B. A., van Dijk, C., and Sands, R. H., *Eur. J. Biochem.* **136,** 201 (1983).
185. van Dijk, C., Mayhew, S. G., Grande, H. J., and Veeger, C., *Eur. J. Biochem.* **102,** 317 (1979).
186. van Dijk, C., Grande, H. J., Mayhew, S. G., and Veeger, C., *Eur. J. Biochem.* **107,** 251 (1980).
187. Filipiak, M., Hagen, W. R., and Veeger, C., *Eur. J. Biochem.* **185,** 547 (1989).
188. Huynh, B. H., Czechowski, M. H., Krüger, H.-J., DerVartanian, D. V., Peck, H. D., Jr., and LeGall, J., *Proc. Natl. Acad. Sci. U.S.A.* **81,** 3728 (1984).
189. Grande, H. J., van Berkel-Arts, A., Bregh, J., van Dijk, K., and Veeger, C., *Eur. J. Biochem.* **131,** 81 (1983).
190. van der Westen, H. M., Mayhew, S. G., and Veeger, C., *FEBS Lett.* **86,** 122 (1978).
191. Hagen, W. R., van Berkel-Arts, A., Kruse-Wolters, K. M., Voorduw, G., and Veeger, C., *FEBS Lett.* **203,** 59 (1986).
192. Patil, D. S., Moura, J. J. G., He, S. H., Teixeira, M., Prickril, B. C., DerVartanian, D. V., Peck, H. D., Jr., LeGall, J., and Huynh, B. H., *J. Biol. Chem.* **263,** 18732 (1988).
193. Spiro, T. G., ed., "Molybdenum Enzymes." Wiley, New York, 1985.